

Quantum error correction against photon loss using multicomponent cat states

Marcel Bergmann and Peter van Loock

Institut für Physik, Johannes Gutenberg-Universität, Staudingerweg 7, 55128 Mainz, Germany

(Received 14 July 2016; published 21 October 2016)

We analyze a generalized quantum error-correction code against photon loss where a logical qubit is encoded into a subspace of a single oscillator mode that is spanned by distinct multicomponent cat states (coherent-state superpositions). We present a systematic code construction that includes the extension of an existing one-photon-loss code to higher numbers of losses. When subject to a photon loss (amplitude damping) channel, the encoded qubits are shown to exhibit a cyclic behavior where the code and error spaces each correspond to certain multiples of losses, half of which can be corrected. As another generalization we also discuss how to protect logical qudits against photon losses, and as an application we consider a one-way quantum communication scheme in which the encoded qubits are periodically recovered while the coherent-state amplitudes are restored as well at regular intervals.

DOI: [10.1103/PhysRevA.94.042332](https://doi.org/10.1103/PhysRevA.94.042332)**I. INTRODUCTION**

Photons are fundamental carriers of quantum information. Traveling at the speed of light, they are the optimal choice for quantum communication. In the form of photonic qubits, each encoded into two orthogonal polarizations, they allow for a simple way to reach any point on a single qubit's Bloch sphere through polarization rotations. Nonetheless, there are also disadvantages when quantum information is encoded into single photons. Two-qubit operations acting jointly on two photons are notoriously hard to achieve and require nonlinear interactions. The biggest drawback for quantum communication, however, is that photons get quickly absorbed along a communication channel such as an optical fiber. This prevents the immediate use of simple photonic qubits for long-distance quantum communication (with distances of 500–1000 km or more).

There have been several proposals of quantum error-correction (QEC) codes to protect photonic qubits against the effect of photon loss [1–3]. Some of these codes make use of an extra number of modes, while each mode contains either zero or one photon [4–6]. Other codes do not require a large number of modes, but instead include the possibility of having more than just one photon in every mode [1]. Yet other loss codes are intermediate in terms of mode and photon number [7]. Among all these codes, in general, the total mean photon number determines the loss scaling of the code: The more photons there are in the encoded states, the more likely some photons will get lost; i.e., the loss rate goes up. On the other hand, for a fixed mode number, the inclusion of more photons leads to larger Hilbert (sub)spaces and the possibility of correcting higher orders of losses. For codewords with a fixed total photon number N , typically $\sqrt{N} - 1$ photon losses can be exactly corrected [1,6,7]. In general, however, there are no simple and efficient schemes to implement such higher-order photonic loss codes.

Another approach to optical, loss-adapted QEC is to encode a logical qubit into a single oscillator mode [8–10]. Such a code can make explicit use of the infinite-dimensional Hilbert space already available with just one optical, physical mode. By sticking to a finite-dimensional (logical qubit) code space, such codes also circumvent existing no-go results for efficient QEC of logical continuous-variable Gaussian states encoded

into physical, multimode Gaussian states [11–15] and subject to Gaussian error channels [16,17]. The qubit-into-oscillator codes are approximate codes based on nonorthogonal codewords that become perfect for infinite squeezing [8] or for infinitely large coherent-state amplitudes [9,10]. Note that the GKP code with codewords as superpositions of position (quadrature) eigenstates [8] is a universal code, whereas the cat code with codewords as even cat states (that is superpositions of even photon numbers) [9,10] is specifically adapted to photon loss errors. Recently, also the concept of an approximate single-mode bosonic code was introduced whose codewords are finite superpositions of certain multiples of the photon number [20].

The possibility of a generalization of the one-loss cat code [9,10] to higher losses has been briefly mentioned a couple of times in the literature (see the Conclusions of Ref. [10] and Sec. 4.2 on page 6 of the Supplementary Information of Ref. [21]), including a few more detailed hints about the conceptual character of such an extension in a very recent publication (Fig. 1 on page 5 and Sec. VIB on page 11 of Ref. [20]). However, as far as we know there is no detailed analysis of a generalized code that includes a complete and systematic definition of the codewords as well as a quantitative performance assessment of the code in a full amplitude-damping channel. Here we present such an analysis. We will give a very compact definition of the codewords in terms of eigenvalue equations, expressed in terms of powers of the mode annihilation operators, for any loss order. This way we will also define the canonical codewords for the respective error spaces which satisfy the same eigenvalue equations, but differ from the code space codewords and the codewords from the other error spaces in their (generalized) number parities. Thus, a certain instance of the cat code (corresponding to a certain coherent-state amplitude α , a certain loss order L , and also a certain logical dimension d for general logical qudits living in the code and error spaces) is defined by two sets of eigenvalue equations: one to determine the space (and hence the error syndrome) and another one to define (together with the former set) the codewords. We will demonstrate that for the right choice of codewords there is no deformation of the initial logical qubit (not even for small coherent-state

amplitudes, in which case, however, the codewords begin to overlap significantly). This no-deformation property results in a rather simple and well structured output density matrix when the encoded state is subject to a complete loss channel. This feature is also similar to the cyclic behavior of the one-loss code in the simplified photon-annihilation (“photon-jump”) error model [9,10], but here extended to higher losses and for the full, physical amplitude-damping channel.

The paper is structured as follows. In Sec. II, we start with a discussion of the known one-loss code [9,10] and its properties when subject to individual photon-loss events as well as its behavior in a full loss channel. A generalization of this code to higher numbers of losses is presented in Sec. III, again including a discussion of its behavior under the two manifestations of photon loss (single loss events and full channel). Coherent-state superpositions with sufficiently many components may also be utilized to encode logical quantum information beyond qubits in so-called qudits [22], and we will determine the conditions for such qudit cat codes adapted to one and more losses of photons in Sec. IV. In Sec. V, as an example for an application and in order to illustrate how the loss codes can be used for a quantum information task, we consider a one-way quantum communication scheme, in which an encoded qubit is sent along a quantum channel while being recovered at regular intervals to preserve the qubit information until the end of the channel. The channel here is assumed to cover a rather long distance (such as 1000 km as a typical distance in long-distance quantum communication), and in addition to the qubit recoveries we also show how the decay of the coherent-state amplitude can be, in principle, dealt with as well for such a large total distance. After the Conclusions we present several appendices that include additional technical details and explanations.

II. ONE-LOSS CAT CODE

It is rather well known that there is a twofold effect when a cat state, i.e., a superposition of two distinct coherent states such as $\propto(|\alpha\rangle + |-\alpha\rangle)$ is subject to a full photon-loss (amplitude-damping) channel. On the one hand, the coherent-state amplitude α in each term is attenuated depending on the channel transmission parameter, $\sqrt{\gamma}\alpha$, corresponding to an exponential amplitude decay with distance. On the other hand, a random phase flip occurs that incoherently mixes the initial cat state with its phase-flipped version, such as $\propto(|\alpha\rangle - |-\alpha\rangle)$, where the flip probability also depends on the channel transmission γ and on the initial amplitude α . In a cat-state qubit encoding [23,24], a loss-induced phase flip of a logical qubit could be corrected when the qubit is encoded into an additional layer of a multiqubit repetition code composed of three or more logical cat qubits (i.e., by adding two or more physical oscillator modes) [3,25,26]. A conceptually more innovative approach, however, would stick to a single oscillator mode and instead exploit more than just two (near-)orthogonal coherent-state components of that mode (i.e., exploiting a manifold with dimension larger than two in the oscillator’s phase space). While it is obvious that this approach enables one to reach higher dimensions, it is not immediately clear how this can provide protection against photon losses. In Refs. [9,10], however, it was shown that

by constructing two (near-)orthogonal codewords, both in the form of even cat states (those with only even photon-number terms), a logical qubit can be encoded that remains intact under the effect of a lost photon, as the qubit is then mapped onto an orthogonal error space that is spanned by two (near-)orthogonal codewords, both in the form of odd cat states (those with only odd photon-number terms).

Formally, for the even cat code given in [9,10], the basic codewords are certain +1 eigenstates of the number parity operator $(-1)^{\hat{n}}$,

$$|\bar{0}_+\rangle = \frac{1}{\sqrt{N_+}}(|\alpha\rangle + |-\alpha\rangle), \quad |\bar{1}_+\rangle = \frac{1}{\sqrt{N_+}}(|i\alpha\rangle + |-i\alpha\rangle), \quad (1)$$

with normalization constant $N_{\pm} = 2 \pm 2 \exp(-2\alpha^2)$ (N_- for later). Throughout we assume $\alpha \in \mathbb{R}$. By writing the coherent states in the Fock basis, one can easily confirm that both codewords have only even photon-number terms,

$$\begin{aligned} |\bar{0}_+\rangle &= \frac{2e^{-\alpha^2/2}}{\sqrt{N_+}} \left(|0\rangle + \frac{\alpha^2}{\sqrt{2}}|2\rangle + \frac{\alpha^4}{2\sqrt{6}}|4\rangle + \dots \right), \\ |\bar{1}_+\rangle &= \frac{2e^{-\alpha^2/2}}{\sqrt{N_+}} \left(|0\rangle - \frac{\alpha^2}{\sqrt{2}}|2\rangle + \frac{\alpha^4}{2\sqrt{6}}|4\rangle - \dots \right). \end{aligned} \quad (2)$$

These two so-called even cat states are, in general, not orthogonal, but for large α , as $e^{-\alpha^2/2}\alpha^k \rightarrow 0$, an infinite superposition of nearly equally weighted even-number states is obtained for each codeword, $|\bar{0}_+\rangle \propto |0\rangle + |2\rangle + |4\rangle + \dots$ and $|\bar{1}_+\rangle \propto |0\rangle - |2\rangle + |4\rangle - \dots$, and thus $\langle \bar{0}_+ | \bar{1}_+ \rangle \approx 0$ (notice the alternating sign in $|\bar{1}_+\rangle$). For general α , their overlap is (see Appendix B)

$$\begin{aligned} \langle \bar{0}_+ | \bar{1}_+ \rangle &= \frac{1}{N_+} (\langle \alpha | i\alpha \rangle + \langle \alpha | -i\alpha \rangle + \langle -\alpha | i\alpha \rangle + \langle -\alpha | -i\alpha \rangle) \\ &= \frac{\cos(\alpha^2)}{\cosh(\alpha^2)}, \end{aligned} \quad (3)$$

which indeed goes to zero in the limit $\alpha \rightarrow \infty$. Instead of the codewords in Eq. (1), as an alternative qubit basis, we may also use the two *orthogonal* states

$$|\bar{0}_+ \pm \bar{1}_+\rangle = \frac{1}{\sqrt{N'_{\pm}}} (|\alpha\rangle + |-\alpha\rangle \pm |i\alpha\rangle \pm |-i\alpha\rangle), \quad (4)$$

which span the same (even) code space as $\{|\bar{0}_+\rangle, |\bar{1}_+\rangle\}$ do and hence represent the same (even) cat code (N'_{\pm} are some normalisation constants). Their exact orthogonality (for any α) can be immediately seen in the Fock basis:

$$\begin{aligned} |\bar{0}_+ + \bar{1}_+\rangle &= \frac{4e^{-\alpha^2/2}}{\sqrt{N'_+}} \left(|0\rangle + \frac{\alpha^4}{2\sqrt{6}}|4\rangle + \frac{\alpha^8}{24\sqrt{70}}|8\rangle + \dots \right), \\ |\bar{0}_+ - \bar{1}_+\rangle &= \frac{4e^{-\alpha^2/2}}{\sqrt{N'_-}} \left(\frac{\alpha^2}{\sqrt{2}}|2\rangle + \frac{\alpha^6}{12\sqrt{5}}|6\rangle \right. \\ &\quad \left. + \frac{\alpha^{10}}{720\sqrt{7}}|10\rangle + \dots \right). \end{aligned} \quad (5)$$

Here we refer to the nonorthogonal codewords $|\bar{0}_+\rangle$ and $|\bar{1}_+\rangle$ as the (approximate) logical Pauli- \bar{Z} basis, and in this sense, the states $|\bar{0}_+ \pm \bar{1}_+\rangle$ can be thought of as a logical Pauli- \bar{X} basis obtained by taking an equally weighted sum or

difference of the two \bar{Z} eigenstates. This is similar to the cat-qubit encoding of Ref. [24] when two nonorthogonal phase-rotated coherent states $\{|\pm\alpha\rangle\}$ form the computational \bar{Z} basis, while the two orthogonal even and odd cat states $\{|\alpha\rangle \pm |-\alpha\rangle\}$ correspond to the Hadamard-transformed, logical \bar{X} basis (this encoding, however, does not represent a loss code that makes it possible to correct a certain nonzero number of photon losses, and it corresponds to the 0th order of our family of generalized cat codes; see next section).

Although $\{|\bar{0}_+\rangle, |\bar{1}_+\rangle\}$ and $\{|\bar{0}_+ \pm \bar{1}_+\rangle\}$ represent the same code, we will see that, nonetheless, the choice of codewords, for example the \bar{Z} or \bar{X} basis, does make a difference when assessing the code's performance in a physical loss channel. This is related to the fact that the code is an approximate code, for which there is not a clear distinction between correctable errors (exactly satisfying the Knill-Laflamme (KL) conditions [27]; see Appendix A) and uncorrectable errors (violating the KL conditions) like for an exact code. For the approximate cat code, those errors that are, in principle, correctable may still give violations of the KL conditions; however, these violations go away in the limit of large amplitudes α . For general α values, it then depends on the choice of codewords as to what particular KL conditions are violated and, as a result, what particular logical errors occur. These logical errors reduce the (input-state-dependent qubit) fidelity, which is further reduced by the uncorrectable errors (which remain uncorrectable even when $\alpha \rightarrow \infty$ and which occur more frequently when α is large; see below).

As one type of violation of the KL conditions can be avoided at least in the 0th order (i.e., the orthogonality condition of the initial codewords) for the basis $\{|\bar{0}_+ \pm \bar{1}_+\rangle\}$, independently of α , it appears beneficial to choose this basis. However, for finite α , these codewords lead to a deformation of the logical qubit; i.e., the norms of the codewords after an otherwise correctable error (such as a one-loss error for the one-loss code) change depending on the specific codeword. This latter effect of qubit deformation turns out to be highly undesirable when the full photon-loss channel is considered and so our choice of codewords will be the nonorthogonal $\{|\bar{0}_+\rangle, |\bar{1}_+\rangle\}$ basis. These codewords do not lead to a qubit deformation; i.e., the change in the norm of either codeword after a one-loss error (or any other correctable error such as 0,4,8,12, . . . or 5,9,13, . . . losses of photons, see below) is independent of the codeword for any α . This no-deformation property of the codewords means that the nice cyclicity feature of the cat code for a simplified, unphysical photon-loss error model, as we discuss next, can be effectively taken over to the physical model of a full loss channel. The only remaining effects that have to be dealt with then come from the nonorthogonality of the codewords $|\bar{0}_+\rangle$ and $|\bar{1}_+\rangle$ before and after an error (i.e., in the code and the error spaces, as it becomes manifest through violations of the corresponding KL conditions). In Appendix B we present a detailed discussion of the KL criteria for the various error models.

In order to understand the behavior of the codewords under photon loss, it is conceptually useful to first model the effects of the channel by individual photon loss and simply apply the annihilation operator \hat{a} to the codewords. Higher losses are analogously represented by higher powers of \hat{a} . It also turns out to be advantageous to look at even and odd powers

separately,

$$\begin{aligned}
 \hat{a}^{2k}|\bar{0}_+\rangle &= \alpha^{2k} \frac{1}{\sqrt{N_+}}(|\alpha\rangle + |-\alpha\rangle), \\
 \hat{a}^{2k}|\bar{1}_+\rangle &= (-1)^k \alpha^{2k} \frac{1}{\sqrt{N_+}}(|i\alpha\rangle + |-i\alpha\rangle), \\
 \hat{a}^{2k+1}|\bar{0}_+\rangle &= \alpha^{2k+1} \frac{1}{\sqrt{N_+}}(|\alpha\rangle - |-\alpha\rangle), \\
 \hat{a}^{2k+1}|\bar{1}_+\rangle &= i(-1)^k \alpha^{2k+1} \frac{1}{\sqrt{N_+}}(|i\alpha\rangle - |-i\alpha\rangle), \quad (6)
 \end{aligned}$$

where $k = 0, 1, 2, \dots$. According to this simplified loss model, a logical qubit of the (unnormalized) form $|\bar{\psi}\rangle = a|\bar{0}_+\rangle + b|\bar{1}_+\rangle$ evolves cyclically into the following four (unnormalized) states [9,10],

$$\begin{aligned}
 |\bar{\psi}\rangle_{4k} &= a|\bar{0}_+\rangle + b|\bar{1}_+\rangle, \\
 |\bar{\psi}\rangle_{4k+1} &= a|\bar{0}_-\rangle + ib|\bar{1}_-\rangle, \\
 |\bar{\psi}\rangle_{4k+2} &= a|\bar{0}_+\rangle - b|\bar{1}_+\rangle, \\
 |\bar{\psi}\rangle_{4k+3} &= a|\bar{0}_-\rangle - ib|\bar{1}_-\rangle, \quad (7)
 \end{aligned}$$

depending on whether the number of lost photons is 0,4,8, . . . or 1,5,9, . . . or 2,6,10, . . . or 3,7,11, . . ., respectively. Here we defined the nonorthogonal basic codewords for the error space as

$$\begin{aligned}
 |\bar{0}_-\rangle &= \frac{1}{\sqrt{N_-}}(|\alpha\rangle - |-\alpha\rangle), \\
 |\bar{1}_-\rangle &= \frac{1}{\sqrt{N_-}}(|i\alpha\rangle - |-i\alpha\rangle), \quad (8)
 \end{aligned}$$

which are two so-called odd cat states with only odd photon-number terms,

$$\begin{aligned}
 |\bar{0}_-\rangle &= \frac{2e^{-\alpha^2/2}\alpha}{\sqrt{N_-}} \left(|1\rangle + \frac{\alpha^2}{\sqrt{6}}|3\rangle + \frac{\alpha^4}{2\sqrt{30}}|5\rangle + \dots \right), \\
 |\bar{1}_-\rangle &= \frac{2e^{-\alpha^2/2}i\alpha}{\sqrt{N_-}} \left(|1\rangle - \frac{\alpha^2}{\sqrt{6}}|3\rangle + \frac{\alpha^4}{2\sqrt{30}}|5\rangle - \dots \right). \quad (9)
 \end{aligned}$$

Again, these two codewords approach an orthogonal qubit basis, this time in the odd-parity error space, when α is sufficiently large (notice the alternating sign in $|\bar{1}_-\rangle$ inherited from $|\bar{1}_+\rangle$). In fact, the overlap between $|\bar{0}_-\rangle$ and $|\bar{1}_-\rangle$ is

$$\begin{aligned}
 \langle \bar{0}_- | \bar{1}_- \rangle &= \frac{1}{N_-} (\langle \alpha | i\alpha \rangle - \langle \alpha | -i\alpha \rangle - \langle -\alpha | i\alpha \rangle + \langle -\alpha | -i\alpha \rangle) \\
 &= \frac{i \sin(\alpha^2)}{\sinh(\alpha^2)}, \quad (10)
 \end{aligned}$$

which again can be made arbitrarily small by increasing α . The code and error spaces can be characterized by their photon-number parity (even/odd) and thus are perfectly distinguishable. However, there can be uncorrectable phase-flip errors of the logical qubit when it is mapped back to the even code space after half a cycle, $|\bar{\psi}\rangle_{4k+2} = a|\bar{0}_+\rangle - b|\bar{1}_+\rangle$, or when it is mapped again onto the odd error space before the end of a cycle, $|\bar{\psi}\rangle_{4k+3} = a|\bar{0}_-\rangle - ib|\bar{1}_-\rangle$. Otherwise, the qubit remains intact either in the code space, $|\bar{\psi}\rangle_{4k} = a|\bar{0}_+\rangle + b|\bar{1}_+\rangle$, or in the error space, $|\bar{\psi}\rangle_{4k+1} = a|\bar{0}_-\rangle + ib|\bar{1}_-\rangle$ (in which case it is transformed by a known and fixed phase gate).

Once the parity is detected, the qubit is recovered and no further correction step is needed. The uncorrectable errors lead to a nonunit fidelity, when the actual physical loss channel is considered, which we do next.

Photon loss, for example occurring in an optical fiber, is described by the amplitude-damping (AD) channel [1]. In the single-mode AD model, the loss of exactly k photons can be expressed by a nonunitary error operator,

$$\begin{aligned} A_k &= \sum_{n=k}^{\infty} \sqrt{\binom{n}{k}} \sqrt{\gamma}^{n-k} \sqrt{1-\gamma}^k |n-k\rangle\langle n| \\ &= \sqrt{\frac{(1-\gamma)^k}{k!}} \sqrt{\gamma}^{\hat{n}} \hat{a}^k, \end{aligned} \quad (11)$$

$\forall k \in \{0, 1, \dots, \infty\}$ and with the number operator $\hat{n} = \hat{a}^\dagger \hat{a}$ in $\sqrt{\gamma}^{\hat{n}}$, which describes the amplitude decay. The probability of losing one photon is $1-\gamma$, which is, for instance, related to the length of the path the photon travels through an optical fiber [28]. Furthermore, note that $\sum_{k=0}^{\infty} A_k^\dagger A_k = \mathbb{1}$. The action of AD on an arbitrary input state ρ is

$$\rho \rightarrow \rho_f = \sum_{k=0}^{\infty} A_k \rho A_k^\dagger. \quad (12)$$

The full loss channel is now a (complete-positive) trace-preserving map that incorporates all possible individual photon-loss events as well as the effect of amplitude decay.

Let us now study the action of AD on the encoding in Eq. (1). The somewhat lengthy calculations are presented in Appendix B and the channel evolution of a normalized logical qubit $|\psi\rangle$ is found to be

$$\begin{aligned} \bar{\rho} &= \tilde{p}_0 \left[\frac{a|\tilde{0}_+\rangle + b|\tilde{1}_+\rangle}{\sqrt{1 + 2 \operatorname{Re}(ab^*) \frac{\cos(\gamma\alpha^2)}{\cosh(\gamma\alpha^2)}}} \right] \times \text{H.c.} \\ &+ \tilde{p}_1 \left[\frac{a|\tilde{0}_-\rangle + ib|\tilde{1}_-\rangle}{\sqrt{1 - 2 \operatorname{Re}(ab^*) \frac{\sin(\gamma\alpha^2)}{\sinh(\gamma\alpha^2)}}} \right] \times \text{H.c.} \\ &+ \tilde{p}_2 \left[\frac{a|\tilde{0}_+\rangle - b|\tilde{1}_+\rangle}{\sqrt{1 - 2 \operatorname{Re}(ab^*) \frac{\cos(\gamma\alpha^2)}{\cosh(\gamma\alpha^2)}}} \right] \times \text{H.c.} \\ &+ \tilde{p}_3 \left[\frac{a|\tilde{0}_-\rangle - ib|\tilde{1}_-\rangle}{\sqrt{1 + 2 \operatorname{Re}(ab^*) \frac{\sin(\gamma\alpha^2)}{\sinh(\gamma\alpha^2)}}} \right] \times \text{H.c.} \end{aligned} \quad (13)$$

The statistical weights in this mixture are given by

$$\begin{aligned} \tilde{p}_0 &= \frac{1 + 2 \operatorname{Re}(ab^*) \frac{\cos(\gamma\alpha^2)}{\cosh(\gamma\alpha^2)}}{1 + 2 \operatorname{Re}(ab^*) \frac{\cos(\alpha^2)}{\cosh(\alpha^2)}} p_0, \\ \tilde{p}_1 &= \frac{1 - 2 \operatorname{Re}(ab^*) \frac{\sin(\gamma\alpha^2)}{\sinh(\gamma\alpha^2)}}{1 + 2 \operatorname{Re}(ab^*) \frac{\cos(\alpha^2)}{\cosh(\alpha^2)}} p_1, \\ \tilde{p}_2 &= \frac{1 - 2 \operatorname{Re}(ab^*) \frac{\cos(\gamma\alpha^2)}{\cosh(\gamma\alpha^2)}}{1 + 2 \operatorname{Re}(ab^*) \frac{\cos(\alpha^2)}{\cosh(\alpha^2)}} p_2, \\ \tilde{p}_3 &= \frac{1 + 2 \operatorname{Re}(ab^*) \frac{\sin(\gamma\alpha^2)}{\sinh(\gamma\alpha^2)}}{1 + 2 \operatorname{Re}(ab^*) \frac{\cos(\alpha^2)}{\cosh(\alpha^2)}} p_3, \end{aligned} \quad (14)$$

where

$$\begin{aligned} p_0 &= \frac{\cosh(\gamma\alpha^2)}{2 \cosh(\alpha^2)} \{\cos[\alpha^2(1-\gamma)] + \cosh[\alpha^2(1-\gamma)]\}, \\ p_1 &= \frac{\sinh(\gamma\alpha^2)}{2 \cosh(\alpha^2)} \{\sin[\alpha^2(1-\gamma)] + \sinh[\alpha^2(1-\gamma)]\}, \\ p_2 &= \frac{\cosh(\gamma\alpha^2)}{2 \cosh(\alpha^2)} \{-\cos[\alpha^2(1-\gamma)] + \cosh[\alpha^2(1-\gamma)]\}, \\ p_3 &= \frac{\sinh(\gamma\alpha^2)}{2 \cosh(\alpha^2)} \{-\sin[\alpha^2(1-\gamma)] + \sinh[\alpha^2(1-\gamma)]\}, \end{aligned} \quad (15)$$

are the loss probabilities for the individual codewords. The states in the mixture above are damped compared to the input states ($\alpha \rightarrow \sqrt{\gamma}\alpha$), which is denoted by the transition $|\tilde{0}_+\rangle \rightarrow |\tilde{0}_+\rangle$, etc., throughout. Although the complex coefficients of the logical input qubit state are normalized as usual, $|a|^2 + |b|^2 = 1$, note that because of the finite overlap between the codewords in the code and error spaces, an extra factor depending on the input qubit state occurs in the statistical weights. This is also related to the fact that the encoding is not an exact quantum error-correction code, but only an approximate one (see Appendix A). The channel output state $\bar{\rho}$ in Eq. (13) still reflects the cyclic behavior of the code [29] under individual photon-loss events owing to the use of the \tilde{Z} -basis codewords for the logical qubit (thus, avoiding its deformation and a resulting mixture of infinitely many deformed qubits corresponding to infinitely many different loss events). The choice of the logical basis becomes irrelevant only when $\alpha \rightarrow \infty$ [30]. Besides the damping of α , an uncorrectable phase flip occurs whenever 2, 6, 10, ... or 3, 7, 11, ... photons are lost. Any other loss errors belong to the correctable set.

The error correction works by a Quantum Non-Demolition measurement (QND)-type parity measurement which distinguishes between even and odd photon numbers. For this encoding, the probability to correctly identify the error syndrome is the sum of the statistical weights of the correctable components in the mixture,

$$F(a, b) = \tilde{p}_0(a, b) + \tilde{p}_1(a, b). \quad (16)$$

The worst-case fidelity F_{wc} is then lower bounded as

$$F_{wc} \geq \min_{a, b} F(a, b) \equiv F. \quad (17)$$

This bound F is the minimum of the total probability of correctable errors over all input states. How this lower bound can be understood is explained in Appendix C.

The bound F for the one-loss cat code [for a balanced logical qubit minimizing $F(a, b)$, see Appendix C] is shown in Fig. 2. The actual F_{wc} is at least as large as plotted there, so that the minimal performance can be inferred. The statistical weights from Eq. (14) are shown in Fig. 1, also for a balanced logical qubit.

III. GENERALIZED CAT CODES

Let us now generalize the one-loss code to include higher losses and state the defining equations for the codewords $|\tilde{0}\rangle$ and $|\tilde{1}\rangle$ of an approximate qubit QEC code that is capable of

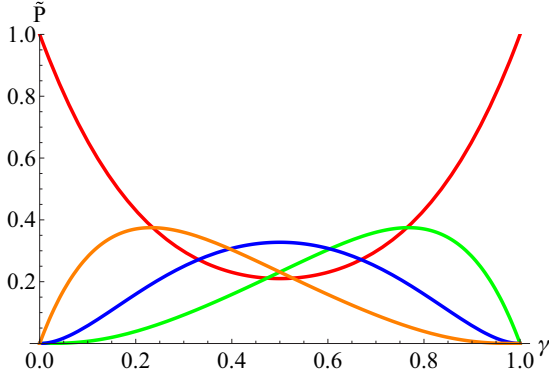


FIG. 1. Statistical weights for $\alpha = 2$ and $a = b = \frac{1}{\sqrt{2}}$ (from top to bottom at $\gamma = 1$): \tilde{p}_0 (red), \tilde{p}_1 (green), \tilde{p}_2 (blue), \tilde{p}_3 (orange) as functions of the damping parameter γ (no damping means $\gamma = 1$). Thus, the red and the green curves represent the weights of the correctable errors (0,4,8, . . . and 1,5,9, . . . losses), while the blue and orange curves correspond to the uncorrectable errors (2,6,10, . . . and 3,7,11, . . . losses). Note that the a, b dependence can lead to a different qualitative behavior of the probabilities for different logical qubits.

correcting L losses:

$$\begin{aligned} \exp\left(\frac{2\pi i \hat{n}}{L+1}\right)|\bar{0}\rangle &= |\bar{0}\rangle, \\ \exp\left(\frac{2\pi i \hat{n}}{L+1}\right)|\bar{1}\rangle &= |\bar{1}\rangle, \\ (\hat{a}^{L+1} - \alpha^{L+1})|\bar{0}\rangle &= 0, \\ (\hat{a}^{L+1} + \alpha^{L+1})|\bar{1}\rangle &= 0. \end{aligned} \quad (18)$$

Here $\hat{n} = \hat{a}^\dagger \hat{a}$ is again the number operator. We will refer to the first two equations as the “parity conditions” that determine the error syndrome and hence the subspace in which the qubit resides after an error occurred (one code space and L error spaces). The current choice of eigenvalue $+1$ for the two parity conditions in Eq. (18) corresponds to (the codewords of) the original code space. The error spaces spanned by two codewords with another parity are described by parity conditions with other phase factors as eigenvalues; see below and Appendix D. This is reminiscent of the stabilizer formalism for QEC in terms of Pauli operators [31]. The last two equations in Eq. (18) define the codewords in every subspace and remain unchanged for different parities (subspaces); i.e., both codewords are always zero eigenstates of the corresponding (generally nonlinear) expressions for the mode operator \hat{a} .

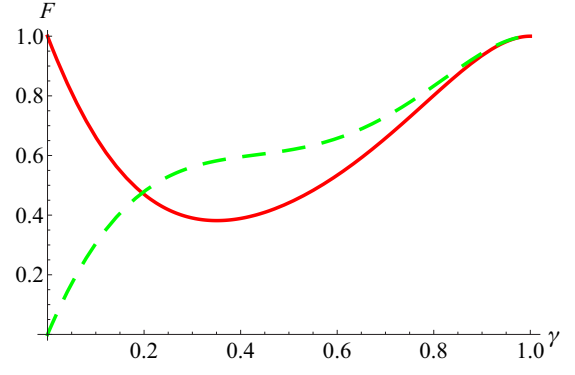


FIG. 2. Probability $F(a, b)$ with a logical qubit $a = b = \frac{1}{\sqrt{2}}$ (red solid line) and $a = -b = \frac{1}{\sqrt{2}}$ (green dashed line) for $\alpha = 2$ as a function of the damping parameter γ (no damping means $\gamma = 1$). The actual lower bound on F_{wc} is given by the minimum of the two curves for each γ .

As shown in Appendix D, the (unnormalized) solutions for general L can be written as superpositions of coherent states,

$$\begin{aligned} |\bar{0}\rangle &= \sum_{k=0}^L \left| \alpha \exp\left(\frac{2k\pi i}{L+1}\right) \right\rangle, \\ |\bar{1}\rangle &= \sum_{k=1}^{L+1} \left| \alpha \exp\left[\frac{(2k-1)\pi i}{L+1}\right] \right\rangle. \end{aligned} \quad (19)$$

For $L = 0$, one obtains the coherent-state encoding $|\bar{0}\rangle = |\alpha\rangle$ and $|\bar{1}\rangle = |-\alpha\rangle$ presented in Refs. [23,24] that provides no intrinsic loss protection. The $L = 1$ case corresponds to the one-loss cat code reviewed in Sec. II. Setting $L = 2$ corresponds to a two-loss code, for which the unnormalized codewords become

$$\begin{aligned} |\bar{0}\rangle &= |\alpha\rangle + \left| \alpha \exp\left(\frac{2\pi i}{3}\right) \right\rangle + \left| \alpha \exp\left(-\frac{2\pi i}{3}\right) \right\rangle, \\ |\bar{1}\rangle &= \left| \alpha \exp\left(\frac{\pi i}{3}\right) \right\rangle + |\alpha \exp(\pi i)\rangle + \left| \alpha \exp\left(-\frac{\pi i}{3}\right) \right\rangle. \end{aligned} \quad (20)$$

These are both superpositions of number terms of multiples of three (see Appendix E). As can easily be checked using the defining equations in Eq. (18), a logical qubit $|\bar{\psi}\rangle = a|\bar{0}\rangle + b|\bar{1}\rangle$ then evolves cyclically under the simplified error model (similar to Sec. II) as

$$\begin{aligned} \hat{a}^{3k}|\bar{0}\rangle &= \alpha^{3k}|\bar{0}\rangle, \quad \hat{a}^{3k}|\bar{1}\rangle = (-1)^k \alpha^{3k}|\bar{1}\rangle, \\ \hat{a}^{3k+1}|\bar{0}\rangle &= \alpha^{3k+1} \left[|\alpha\rangle + \exp\left(\frac{2\pi i}{3}\right) \left| \alpha \exp\left(\frac{2\pi i}{3}\right) \right\rangle + \exp\left(-\frac{2\pi i}{3}\right) \left| \alpha \exp\left(-\frac{2\pi i}{3}\right) \right\rangle \right], \\ \hat{a}^{3k+1}|\bar{1}\rangle &= (-1)^k \alpha^{3k+1} \exp\left(\frac{\pi i}{3}\right) \left[\left| \alpha \exp\left(\frac{\pi i}{3}\right) \right\rangle + \exp\left(\frac{2\pi i}{3}\right) \left| \alpha \exp(\pi i) \right\rangle + \exp\left(-\frac{2\pi i}{3}\right) \left| \alpha \exp\left(-\frac{\pi i}{3}\right) \right\rangle \right], \\ \hat{a}^{3k+2}|\bar{0}\rangle &= \alpha^{3k+2} \left[|\alpha\rangle + \exp\left(-\frac{2\pi i}{3}\right) \left| \alpha \exp\left(\frac{2\pi i}{3}\right) \right\rangle + \exp\left(\frac{2\pi i}{3}\right) \left| \alpha \exp\left(-\frac{2\pi i}{3}\right) \right\rangle \right], \\ \hat{a}^{3k+2}|\bar{1}\rangle &= (-1)^k \alpha^{3k+2} \exp\left(\frac{2\pi i}{3}\right) \left[\left| \alpha \exp\left(\frac{\pi i}{3}\right) \right\rangle + \exp\left(-\frac{2\pi i}{3}\right) \left| \alpha \exp(\pi i) \right\rangle + \exp\left(\frac{2\pi i}{3}\right) \left| \alpha \exp\left(-\frac{\pi i}{3}\right) \right\rangle \right], \end{aligned} \quad (21)$$

where again $k = 0, 1, 2, \dots$. Similar to $L = 1$, we encounter a cyclic behavior. For even k (especially $k = 0$ corresponding to 0, 1, and 2 losses), there are no k -dependent phase flips [the factors $(-1)^k$ in front of the transformed $|\bar{1}\rangle$ codewords in lines 1, 3, and 5 on the right-hand side of Eq. (21); see also below] and only fixed, k -independent phase factors (in front of the transformed $|\bar{1}\rangle$ codewords). The parities for the one- and two-loss cases change compared to the zero-loss case from 0, 3, 6, \dots to 2, 5, 8, \dots and 1, 4, 7, \dots , respectively (see Appendix E).

The calculations for the complete, physical AD channel are presented in Appendix E. Besides the basic codewords in the initial code space, we define the (unnormalized) codewords in all the three orthogonal subspaces (one code space and two error spaces for one- and two-photon losses, etc.) as

$$\begin{aligned}
|\bar{0}_0\rangle_2 &= |\alpha\rangle + \left| \alpha \exp\left(\frac{2\pi i}{3}\right) \right\rangle + \left| \alpha \exp\left(-\frac{2\pi i}{3}\right) \right\rangle, \\
|\bar{1}_0\rangle_2 &= \left| \alpha \exp\left(\frac{\pi i}{3}\right) \right\rangle + \left| \alpha \exp(\pi i) \right\rangle + \left| \alpha \exp\left(-\frac{\pi i}{3}\right) \right\rangle, \\
|\bar{0}_1\rangle_2 &= |\alpha\rangle + \exp\left(\frac{2\pi i}{3}\right) \left| \alpha \exp\left(\frac{2\pi i}{3}\right) \right\rangle + \exp\left(-\frac{2\pi i}{3}\right) \left| \alpha \exp\left(-\frac{2\pi i}{3}\right) \right\rangle, \\
|\bar{1}_1\rangle_2 &= \left| \alpha \exp\left(\frac{\pi i}{3}\right) \right\rangle + \exp\left(\frac{2\pi i}{3}\right) \left| \alpha \exp(\pi i) \right\rangle + \exp\left(-\frac{2\pi i}{3}\right) \left| \alpha \exp\left(-\frac{\pi i}{3}\right) \right\rangle, \\
|\bar{0}_2\rangle_2 &= |\alpha\rangle + \exp\left(-\frac{2\pi i}{3}\right) \left| \alpha \exp\left(\frac{2\pi i}{3}\right) \right\rangle + \exp\left(\frac{2\pi i}{3}\right) \left| \alpha \exp\left(-\frac{2\pi i}{3}\right) \right\rangle, \\
|\bar{1}_2\rangle_2 &= \left| \alpha \exp\left(\frac{\pi i}{3}\right) \right\rangle + \exp\left(-\frac{2\pi i}{3}\right) \left| \alpha \exp(\pi i) \right\rangle + \exp\left(\frac{2\pi i}{3}\right) \left| \alpha \exp\left(-\frac{\pi i}{3}\right) \right\rangle.
\end{aligned} \tag{22}$$

Here we introduced the notation $\{|\bar{0}_q\rangle_L, |\bar{1}_q\rangle_L\}$ to specify the order of the loss code (L) and the corresponding error space (q) ($q = 0$ for no loss, $q = 1$ for one-photon loss, and $q = 2$ for two-photon loss, plus cyclic loss events; see below). With these definitions for the canonical codewords in the code and error spaces, Eq. (21) simplifies to

$$\begin{aligned}
\hat{a}^{3k} |\bar{0}_0\rangle_2 &= \alpha^{3k} |\bar{0}_0\rangle_2, & \hat{a}^{3k} |\bar{1}_0\rangle_2 &= (-1)^k \alpha^{3k} |\bar{1}_0\rangle_2, \\
\hat{a}^{3k+1} |\bar{0}_0\rangle_2 &= \alpha^{3k+1} |\bar{0}_1\rangle_2, \\
\hat{a}^{3k+1} |\bar{1}_0\rangle_2 &= (-1)^k \alpha^{3k+1} \exp\left(\frac{\pi i}{3}\right) |\bar{1}_1\rangle_2, \\
\hat{a}^{3k+2} |\bar{0}_0\rangle_2 &= \alpha^{3k+2} |\bar{0}_2\rangle_2, \\
\hat{a}^{3k+2} |\bar{1}_0\rangle_2 &= (-1)^k \alpha^{3k+2} \exp\left(\frac{2\pi i}{3}\right) |\bar{1}_2\rangle_2.
\end{aligned} \tag{23}$$

As shown in Appendix E, a logical qubit $a|\bar{0}_0\rangle_2 + b|\bar{1}_0\rangle_2$ subject to AD becomes a mixture of six components, which can be cast in the form (omitting proper normalizations of the qubits)

$$\begin{aligned}
\bar{\rho} &= p_0(a|\tilde{0}_0\rangle_2 + b|\tilde{1}_0\rangle_2) \times \text{H.c.} \\
&+ p_1(a|\tilde{0}_1\rangle_2 + e^{\frac{i\pi}{3}} b|\tilde{1}_1\rangle_2) \times \text{H.c.} \\
&+ p_2(a|\tilde{0}_2\rangle_2 + e^{\frac{2i\pi}{3}} b|\tilde{1}_2\rangle_2) \times \text{H.c.} \\
&+ p_3(a|\tilde{0}_0\rangle_2 - b|\tilde{1}_0\rangle_2) \times \text{H.c.} \\
&+ p_4(a|\tilde{0}_1\rangle_2 - e^{\frac{i\pi}{3}} b|\tilde{1}_1\rangle_2) \times \text{H.c.} \\
&+ p_5(a|\tilde{0}_2\rangle_2 - e^{\frac{2i\pi}{3}} b|\tilde{1}_2\rangle_2) \times \text{H.c.}
\end{aligned} \tag{24}$$

Recall again the additional damping of the amplitude due to the AD channel ($\alpha \rightarrow \sqrt{\gamma}\alpha$) and correspondingly the adapted notation $\{|\bar{0}_q\rangle_2, |\bar{1}_q\rangle_2\} \rightarrow \{|\tilde{0}_q\rangle_2, |\tilde{1}_q\rangle_2\}$ for $q = 0, 1, 2$. Now the first three terms in Eq. (24) correspond to correctable

logical qubits with, besides some fixed phase gates for $q = 1$ and $q = 2$, photon number parities of 0, 3, 6, \dots or 2, 5, 8, \dots or 1, 4, 7, \dots corresponding to the loss of 0, 6, 12, \dots ($q = 0$) or 1, 7, 13, \dots ($q = 1$) or 2, 8, 14, \dots ($q = 2$) photons, respectively. The additional terms each mix in uncorrectable phase-flip errors for every subspace corresponding to the loss of 3, 9, 15, \dots or 4, 10, 16, \dots or 5, 11, 17, \dots photons. Again, like for the one-loss code, the cyclic behavior of the simplified model is recovered for the full channel (for more details, see Appendix E). Thus, for the $L = 2$ case, among the dominating loss errors, those from one- and two-photon losses can be corrected (i.e., the qubit is still intact in the corresponding error space), whereas those from three-, four-, and five-photon losses cannot (i.e., the qubit is subject to a phase error). For six- and higher-photon losses, the cycle starts again. In general, an L code can correct up to L photon losses plus other cycles and each codeword has $(L + 1)$ coherent-state components living in a $2(L + 1)$ -dimensional manifold.

The lowest cat codes $L = 0, 1, 2, 3$ encoding a logical qubit are illustrated in Fig. 3. In Figs. 4 and 5, the statistical weights and the fidelity bound on F_{wc} , respectively, are shown as functions of the damping (loss) parameter γ .

IV. EXTENSION TO QUDIT CODES

Another generalization that goes beyond the qubit codes presented in the last section is to define equations for the encoding of an arbitrary qudit of d dimensions:

$$\begin{aligned}
\exp\left(\frac{2\pi i \hat{n}}{L+1}\right) |\bar{k}\rangle &= |\bar{k}\rangle, \\
\left[\hat{a}^{L+1} - \exp\left(\frac{2\pi i k}{d}\right) \alpha^{L+1} \right] |\bar{k}\rangle &= 0 \quad \text{for} \\
k &= 0, 1, \dots, d-1.
\end{aligned} \tag{25}$$

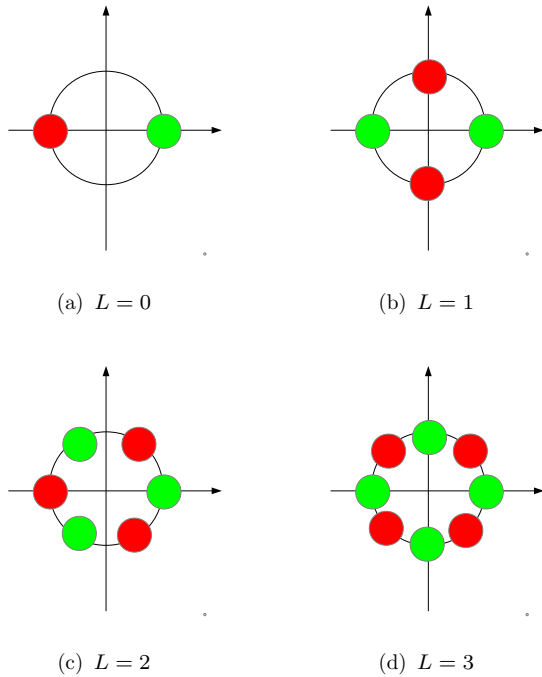


FIG. 3. Illustration of the lowest qubit ($d = 2$) loss codes in phase space. The binary codewords are represented by green ($|\bar{0}\rangle$) and red ($|\bar{1}\rangle$) circles which are to be superimposed.

For $d = 2$, Eq. (18) for logical qubits is obtained. The simplest encoding for general d with $L = 0$ corresponds to $|\bar{k}\rangle = |\alpha e^{\frac{2\pi i k}{d}}\rangle$ for $k = 0, 1, \dots, d - 1$, which is referred to as “coherent states on a ring” in Ref. [22] (see Fig. 6).

For $d = 3$ and $L = 1$, i.e., the simplest loss code beyond $d = 2$, one finds the (unnormalized) solutions

$$\begin{aligned} |\bar{0}\rangle &\equiv |\bar{0}_+\rangle = |\alpha\rangle + |-\alpha\rangle, \\ |\bar{1}\rangle &\equiv |\bar{1}_+\rangle = |e^{\frac{i\pi}{3}}\alpha\rangle + |-e^{\frac{i\pi}{3}}\alpha\rangle, \\ |\bar{2}\rangle &\equiv |\bar{2}_+\rangle = |e^{-\frac{i\pi}{3}}\alpha\rangle + |-e^{-\frac{i\pi}{3}}\alpha\rangle. \end{aligned} \tag{26}$$

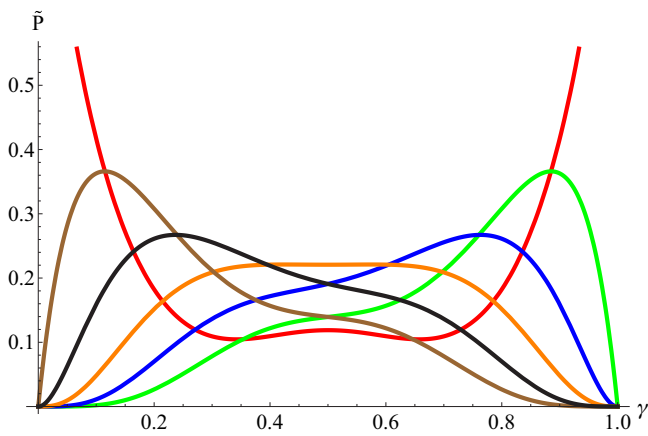


FIG. 4. Statistical weights with $\alpha = 3$ and $a = b = \frac{1}{\sqrt{2}}$ for $L = 2$ (from top to bottom at $\gamma = 1$): \tilde{p}_0 (red), \tilde{p}_1 (green), \tilde{p}_2 (blue), \tilde{p}_3 (orange), \tilde{p}_4 (black), \tilde{p}_5 (brown) as functions of γ . Note that the a, b dependence can lead to a different qualitative behavior of the probabilities for different logical qubits.

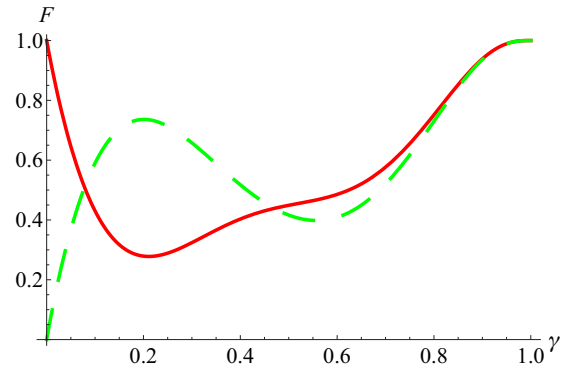


FIG. 5. Probability $F(a, b)$ as a function of γ for $\alpha = 3$ with $a = b = \frac{1}{\sqrt{2}}$ (red, solid line) and $a = -b = \frac{1}{\sqrt{2}}$ (green, dashed line), where $L = 2$. The actual lower bound on F_{wc} is given by the minimum of the two curves for each γ .

The three-dimensional code space is spanned by three (generally nonorthogonal) even cat states, similar to the $L = 1$ qubit code which has two even cat states as codewords. In the simplified error model, we also find a similar cyclic behavior

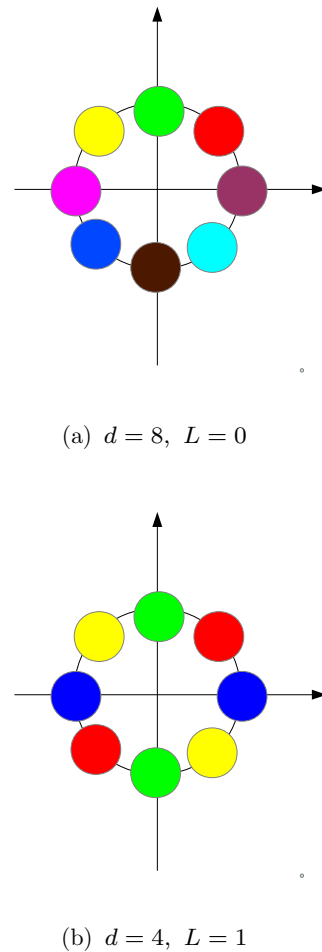


FIG. 6. Illustration of some qudit codes in phase space realized through coherent-state superpositions (every color indicates another codeword) with in total eight components (for $d = 2, L = 3$; see Fig. 2).

of the codewords,

$$\begin{aligned}
 \hat{a}^{2k}|\bar{0}\rangle &= \alpha^{2k}|\bar{0}_+\rangle, \\
 \hat{a}^{2k}|\bar{1}\rangle &= \exp\left(\frac{i\pi}{3}\right)^{2k} \alpha^{2k}|\bar{1}_+\rangle, \\
 \hat{a}^{2k}|\bar{2}\rangle &= \exp\left(-\frac{i\pi}{3}\right)^{2k} \alpha^{2k}|\bar{2}_+\rangle, \\
 \hat{a}^{2k+1}|\bar{0}\rangle &= \alpha^{2k+1}|\bar{0}_-\rangle, \\
 \hat{a}^{2k+1}|\bar{1}\rangle &= \exp\left(\frac{i\pi}{3}\right)^{2k+1} \alpha^{2k+1}|\bar{1}_-\rangle, \\
 \hat{a}^{2k+1}|\bar{2}\rangle &= \exp\left(-\frac{i\pi}{3}\right)^{2k+1} \alpha^{2k+1}|\bar{2}_-\rangle,
 \end{aligned} \tag{27}$$

where $|\bar{0}_-\rangle = |\alpha\rangle - |-\alpha\rangle$, $|\bar{1}_-\rangle = |e^{i\pi/3}\alpha\rangle - |e^{-i\pi/3}\alpha\rangle$, and $|\bar{2}_-\rangle = |e^{-i\pi/3}\alpha\rangle - |e^{i\pi/3}\alpha\rangle$. Depending on the number of lost photons $m = 0, 1, 2, 3, 4, 5$, the logical qudit $a|\bar{0}\rangle + b|\bar{1}\rangle + c|\bar{2}\rangle$ suffers from random relative phases [the phase factors $(e^{\pm i\pi/3})^{2k}$ in front of the transformed codewords $|\bar{1}_\pm\rangle$ and $|\bar{2}_\pm\rangle$]. In fact, only for $k = 0, 3, 6, \dots$ no phase errors occur and a fixed phase gate (the phase factor $e^{\pm i\pi/3}$ in front of $|\bar{1}_-\rangle$ and $|\bar{2}_-\rangle$) is either applied (1, 7, 13, ... losses) or not (0, 6, 12, ... losses). Subject to the full AD channel, the mixed output state for a logical qutrit $a|\bar{0}\rangle + b|\bar{1}\rangle + c|\bar{2}\rangle$ has six components,

$$\begin{aligned}
 |\bar{\psi}_0\rangle &= a|\bar{0}_+\rangle + b|\bar{1}_+\rangle + c|\bar{2}_+\rangle, \\
 |\bar{\psi}_1\rangle &= a|\bar{0}_-\rangle + b \exp\left(\frac{i\pi}{3}\right)|\bar{1}_-\rangle + c \exp\left(-\frac{i\pi}{3}\right)|\bar{2}_-\rangle, \\
 |\bar{\psi}_2\rangle &= a|\bar{0}_+\rangle + b \exp\left(\frac{2i\pi}{3}\right)|\bar{1}_+\rangle + c \exp\left(-\frac{2i\pi}{3}\right)|\bar{2}_+\rangle, \\
 |\bar{\psi}_3\rangle &= a|\bar{0}_-\rangle - b|\bar{1}_-\rangle - c|\bar{2}_-\rangle, \\
 |\bar{\psi}_4\rangle &= a|\bar{0}_+\rangle - b \exp\left(\frac{i\pi}{3}\right)|\bar{1}_+\rangle - c \exp\left(-\frac{i\pi}{3}\right)|\bar{2}_+\rangle, \\
 |\bar{\psi}_5\rangle &= a|\bar{0}_-\rangle - b \exp\left(\frac{2i\pi}{3}\right)|\bar{1}_-\rangle - c \exp\left(-\frac{2i\pi}{3}\right)|\bar{2}_-\rangle,
 \end{aligned} \tag{28}$$

with some statistical weights. Here only $|\bar{\psi}_0\rangle$ and $|\bar{\psi}_1\rangle$ correspond to correctable qutrits (corresponding to 0, 6, 12, ... and 1, 7, 13, ... losses, respectively). All the remaining qutrits $|\bar{\psi}_2\rangle$, $|\bar{\psi}_3\rangle$, $|\bar{\psi}_4\rangle$, and $|\bar{\psi}_5\rangle$ have suffered from phase errors (corresponding to 2, 8, 14, ... or 3, 9, 15, ... or 4, 10, 16, ... or 5, 11, 17, ... losses, respectively). With six losses a new cycle starts.

In general, for a general L code the period of a cycle depends on the total number of coherent-state components of the code [that is $d(L + 1)$], e.g., a four cycle (i.e., four terms in $\bar{\rho}$) for $d = 2|L = 1$ or a six cycle (six terms in $\bar{\rho}$) for both $d = 2|L = 2$ and $d = 3|L = 1$.

V. APPLICATION IN A ONE-WAY QUANTUM COMMUNICATION SCHEME

Loss-adapted quantum error-correction codes are a key ingredient for a so-called third-generation quantum repeater [6]. In such a third-generation quantum repeater, the goal is

to transmit an encoded qubit over a total distance \mathcal{L} without distributing, as an initial step, entangled states over smaller segments of the entire channel like in a more standard quantum repeater (i.e., either a first-generation repeater based on entanglement purification and swapping [32,33] or a second-generation one that includes quantum error correction of local errors [34]). Nonetheless, also in a third-generation repeater, the total distance \mathcal{L} is divided into smaller elementary distances $L_0 < \mathcal{L}$ and at each distance L_0 a repeater station is placed. However, at every repeater station, quantum error correction (especially in order to suppress the photon transmission loss) is performed on an incoming qubit which has traveled over the distance L_0 . The recovered logical qubit is then sent further to the next station and so on until it reaches the final repeater station. Thus, in a third-generation repeater, there is no need to temporarily store entangled states until neighboring entangled states have been distributed and purified, and there is also no need to send classical information back and forth between repeater stations. Such two-way classical communication slows down the repeater (and hence reduces the rate) and it also makes good quantum memories a necessity. In contrast, a third-generation repeater only requires one-way classical communication and, in principle, no quantum memories are needed at all. Quantum information is sent directly at rates that approach, in principle, those achievable in classical communication. As loss-protected qubits are usually encoded into multimode states [6], an attractive feature of the cat loss code would be that only a single optical mode must be sent.

In the case of cat codes, the first step at each repeater station is a QND-type parity measurement that determines the corresponding error space. After fixing the parity, the logical state is recovered to a great extent and the initial logical qubit resides in some error space with high, but nonunit fidelity.

As mentioned in the former sections, a special problem that occurs with the transmission of cat-code qubits is the distance-dependent damping of the amplitude. In addition to the qubit recovery (QR) at each repeater station, the amplitude has to be restored as well. A probabilistic scheme for this amplitude restoration (AR) is presented in Appendix F. In our AR scheme, we use quantum teleportation and choose to teleport the qubit back into the code space, while restoring the amplitude. A schematic is depicted in Fig. 7(a). After each repeater station, the qubit is recovered as well as the amplitude

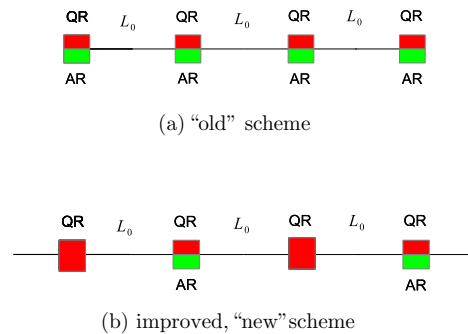


FIG. 7. Schematic of a one-way quantum repeater with qubit recovery (QR, red) as well as amplitude restoration (AR, green) at every repeater station (a) or with QR at every repeater station and AR only at every second station (b).

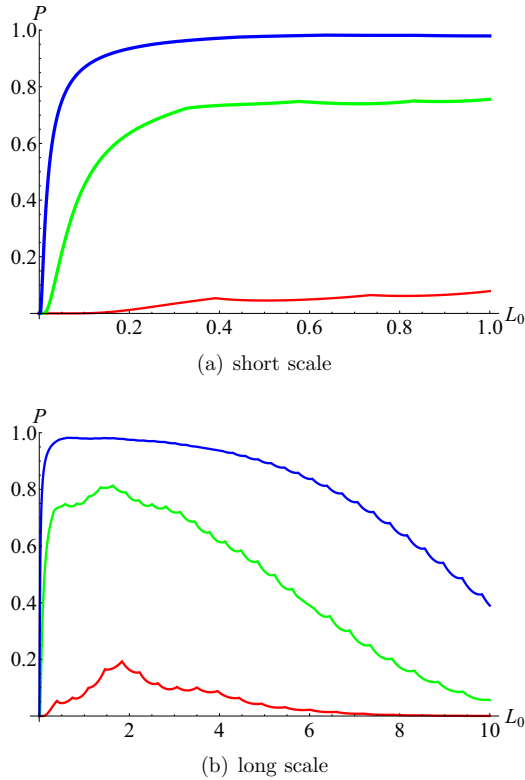


FIG. 8. Total success probability P of amplitude restoration as a function of the elementary distance L_0 (in km) in an improved (“new”) one-way scheme over a total distance of 1000 km for $L = 4$ and various α (from top to bottom): $\alpha = 8$ (blue), $\alpha = 7$ (green), $\alpha = 6$ (red).

is restored. Figure 7(b) shows an improved scheme in which the qubit is still recovered at each repeater station, but the amplitude is restored at every second repeater station only. The total success probability for this improved scheme is shown in Fig. 8. One observes that the total success probability initially increases with the elementary distance L_0 before reaching a maximum and tending to zero again. Indeed, doing AR at the end of the total channel at distance \mathcal{L} corresponds to an exponentially small success probability, while a scheme in which AR is performed too frequently also means that the probabilistic element introduced via AR accumulates over the total distance. We expect that a further improvement compared to the results shown in Fig. 8 can be obtained by doing AR even less frequently than at every second repeater station. Here we shall only demonstrate an in-principle improvement when QR and AR are not always performed synchronously, without intending to find an optimal scheme. The fidelity bound

$$F = \left\{ \min_{a,b} [\tilde{p}_0(a,b) + \tilde{p}_1(a,b) + \dots + \tilde{p}_L(a,b)] \right\}^{\mathcal{L}/L_0}, \quad (29)$$

however, is near unity for short elementary distances and decreases with increasing L_0 (see Fig. 9). Note that this bound does not include those events (occurring with probabilities $\tilde{p}_{L+1}, \dots, \tilde{p}_{2L+1}$) where the qubit gets “self-corrected” after a suitable sequence of uncorrectable errors.

To summarize, qubit recovery is necessary after sufficiently short distances, whereas amplitude restoration seems to be

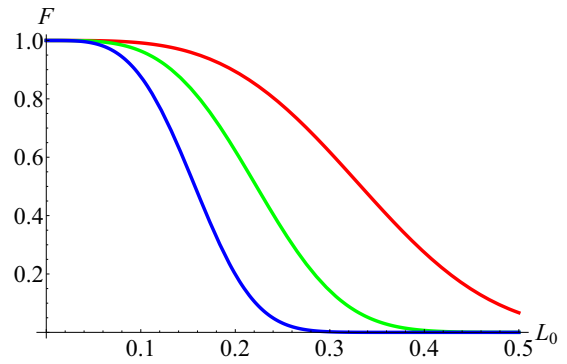


FIG. 9. Bound F on worst-case fidelity as a function of the elementary distance L_0 (in km) for a one-way scheme over a total distance of 1000 km with $L = 4$ for various α (from top to bottom): $\alpha = 6$ (red), $\alpha = 7$ (green), $\alpha = 8$ (blue).

beneficial after longer but not too-long distances. That the logical qubits must be recovered frequently after short distances is also expected, since the loss code does not tolerate too-large losses for the quantum information to remain intact. A comparison of the success probabilities and fidelities for the “old” and the improved “new” scheme with different cat codes and different amplitudes is shown in Tables I–III. Besides the significantly higher success probabilities, the improved scheme also gives slightly better fidelities.

In general, the expected trade-off is recovered: For too-large amplitudes α , the photon-loss probability goes up (and hence the fidelity decreases), while the codewords become more orthogonal [and hence the filter probabilities (see Appendix F) and thus the AR probabilities increase]. Conversely, for smaller α , the AR becomes less likely to succeed, while larger fidelities can be obtained. A nontrivial result is to find a code L and a protocol, for which an α regime exists that allows for both reasonable success probabilities ($\sim 1\%$ – 10%) and near-unit fidelities at some elementary distances L_0 . For $L = 3$ using the old scheme such an α regime does not seem to exist (see Table I). With the new, improved scheme, however, the

TABLE I. Comparison between the “old” and the “new” schemes for a total distance of $\mathcal{L} = 1000$ km with the $L = 3$ code, L_0 in km. Color indicates near-feasible regimes. Here, “ ≈ 0 ” corresponds to $\lesssim 10^{-100}$.

α	L_0	F_{new}	P_{new}	F_{old}	P_{old}
4.0	0.01	0.999 989 00	≈ 0	0.999 989	≈ 0
4.0	0.10	0.989 446 00	≈ 0	0.989 275	10^{-76}
4.0	1.00	0.004 739 19	3×10^{-8}	0.002 325 37	10^{-12}
4.5	0.01	0.999 970 00	≈ 0	0.999 97	10^{-42}
4.5	0.10	0.973 278 00	0.008 308 84	0.972 789	7×10^{-5}
4.5	1.00	9×10^{-6}	0.008 806 18	10^{-6}	3×10^{-3}
5.0	0.01	0.999 931 00	≈ 0	0.999 931	10^{-67}
5.0	0.10	0.940 122 00	5×10^{-4}	0.876 04	2×10^{-7}
5.0	1.00	≈ 0	0.168 942 00	6×10^{-22}	0.084 745 3
6.0	0.01	0.999 706 00	5×10^{-4}	0.999 705	3×10^{-7}
6.0	0.10	0.774 627 00	0.468 715 00	0.771 153	0.221 926
6.0	1.00	≈ 0	0.893 489 00	3×10^{-36}	0.843 821

TABLE II. Comparison between the “old” and the “new” schemes for a total distance of $\mathcal{L} = 1000$ km with the $L = 4$ code, L_0 in km. Color indicates feasible regimes.

α	L_0	F_{new}	P_{new}	F_{old}	P_{old}
6	0.01	0.999 999	3×10^{-31}	0.999 999	10^{-61}
6	0.1	0.991 757	4×10^{-4}	0.991 574	4×10^{-7}
6	1.00	10^{-9}	0.078 741 8	4×10^{-11}	0.045 532 9
7	0.01	0.999 996	6×10^{-4}	0.999 996	3×10^{-7}
7	0.1	0.963 915	0.451 687	0.963 14	0.214 877
7	1.00	6×10^{-28}	0.755 955	3×10^{-22}	0.740854
8	0.01	0.999 983	0.230 988	0.999 983	0.053 100 4
8	0.1	0.876 309	0.867 937	0.873 809	0.749 01
8	1.00	10^{-66}	0.979 637	10^{-75}	0.977 982

$L = 3$ code may suffice for elementary distances of $L_0 \sim 100$ m. For the $L = 4$ and $L = 5$ codes, both schemes can work at elementary distances of $L_0 \sim 10$ – 100 m. A general observation is that elementary distances as large as ~ 1 km result in very bad fidelities. Thus, a cat-encoded logical qubit is more sensitive to too-large losses and too-large L_0 than, for instance, a single-photon-based, multimode, quantum parity code (QPC)-encoded qubit for which $L_0 \sim 1$ km works [6,35]. However, the fact that a cat-encoded qubit only requires a single optical mode means that low success probabilities in a single repeater chain could be efficiently compensated via (e.g., broadband) parallelization or multiplexing.

VI. CONCLUSIONS

We analysed a generalized quantum error-correction code that is adapted to correct errors induced from photon losses and is based on superpositions of coherent states. Our generalization includes instances of such a cat code where errors from more than one-photon loss can be, in principle, approximately corrected. For the higher-loss codes, however, the overlap of the codewords increases and must be compensated by an increasing coherent-state amplitude which results in a growing error rate. Thus, one encounters the usual trade-

TABLE III. Comparison between the “old” and the “new” schemes for a total distance of $\mathcal{L} = 1000$ km with the $L = 5$ code, L_0 in km. Color indicates feasible regimes. Here, “ ≈ 0 ” corresponds to $\lesssim 10^{-100}$.

α	L_0	F_{new}	P_{new}	F_{old}	P_{old}
6	0.01	1	≈ 0	1	≈ 0
6	0.1	0.999 781	4×10^{-24}	0.999 776	10^{-47}
6	1.00	0.006 392 87	3×10^{-5}	3×10^{-3}	6×10^{-6}
7	0.01	1	3×10^{-50}	1	≈ 0
7	0.1	0.998 659	10^{-5}	0.998 624	10^{-10}
7	1.00	2×10^{-9}	0.066 15	$4 \cdot 10^{-11}$	0.075 974 7
8	0.01	1	10^{-7}	1	2×10^{-14}
8	0,1	0.993 71	0.194 448	0.993 546	0.041 740 6
8	1.00	4×10^{-27}	0.691 036	10^{-31}	0.659 869
9	0.01	1	4×10^{-3}	1	1.75×10^{-5}
9	0.1	0.975 983	0.578 119	0.975 37	0.334 447
9	1.00	5×10^{-64}	0.963 224	4×10^{-74}	0.891 03

offs when a continuous-variable encoding is employed. We illustrate such an effect for the example of a one-way quantum communication scheme for large distances based on cat codes.

The nonorthogonality of the codewords could be entirely avoided by choosing a particular logical basis in the code space (the \tilde{X} instead of the \tilde{Z} basis); however, this would be at the expense of a deformation of the logical qubits for finite coherent-state amplitudes leading to a complicated and undesirable output density matrix. Our choice of the \tilde{Z} basis circumvents this deformation at the expense of nonzero codeword overlap.

Another generalization that we discussed for cat codes is for a higher-dimensional code space beyond logical qubits, i.e., qudits. Future work will aim at potential optical implementations of these codes, including practical ways to encode, to do the measurements (parity detections), and to achieve the coherent-state amplitude restorations (either by creating the encoded, entangled ancilla states, as proposed here, or by employing an alternative method).

ACKNOWLEDGMENT

We acknowledge support from Q.com (BMBF) and Hipercom (ERA-NET CHISTERA).

APPENDIX A: KNILL-LAFLAMME CONDITIONS FOR QEC

Decoherence is a usually undesired quantum effect that prevents a quantum system from a purely unitary evolution. One method to overcome decoherence is the usage of a quantum error-correction code. A quantum error-correction code is a d -dimensional subspace of some higher-dimensional Hilbert space. The d basis vectors $\{|c_1\rangle, |c_2\rangle, \dots, |c_d\rangle\}$ are referred to as codewords and any normalized superposition corresponds to a logical or an encoded qubit.

Given an explicit error model with error operators E_i , it can be shown that the action of certain error operators from the so-called correctable set can be reversed by means of a recovery operation, if and only if the following two sets of conditions are fulfilled. The first set of condition states that corrupted codewords are orthogonal

$$\langle c_k | E_i^\dagger E_j | c_l \rangle = 0 \quad \text{if } k \neq l, \quad (\text{A1})$$

which partially incorporates the quantum mechanical requirement for distinguishability of the different code and error spaces. The second one includes the nondeformability condition, i.e.,

$$\langle c_l | E_i^\dagger E_i | c_l \rangle = g_i, \quad \forall l, \quad (\text{A2})$$

which states that the norm of corrupted state only depends on the error and not on the codeword. These two sets of conditions are referred to as the Knill-Laflamme conditions. An encoding that exactly fulfills the KL conditions for a set of errors is called an exact code and the corresponding set is the correctable error set.

In optical quantum information, the main mechanism of decoherence is photon loss, as described in Sec. II. In this context, the notion of approximate quantum error-correction codes has been introduced [4]. In an approximate QEC for AD,

the KL conditions are only fulfilled up to a certain order in the loss parameter $1 - \gamma$; thus, orthogonality and nondeformability are not strictly fulfilled. In the context of the present cat codes, it also depends on the amplitude α whether the KL conditions are fulfilled or not.

APPENDIX B: FULL LOSS CHANNEL AND KL CONDITIONS FOR THE ONE-LOSS CAT CODE

Let us first consider the simplified set of errors $\mathcal{E} = \{\hat{a}^{4k}, \hat{a}^{4k+1}, k \in \mathbb{N}_0\}$. For the even-cat codewords of Eq. (1) (i.e., the “ \bar{Z} basis”), we have the following KL conditions:

$$\begin{aligned}
 \langle \bar{0}_+ | (\hat{a}^{4k})^\dagger \hat{a}^{4k} | \bar{1}_+ \rangle &= i^{4k} (\alpha^2)^{4k} \frac{1}{\sqrt{N_+}} (\langle \alpha | + \langle -\alpha |) \frac{1}{\sqrt{N_+}} (|i\alpha\rangle + | -i\alpha\rangle) \\
 &= \frac{(\alpha^2)^{4k}}{N_+} (\langle \alpha | i\alpha\rangle + \langle \alpha | -i\alpha\rangle + \langle -\alpha | i\alpha\rangle + \langle -\alpha | -i\alpha\rangle) \\
 &= \frac{(\alpha^2)^{4k}}{N_+} [\exp(-\alpha^2) \exp(i\alpha^2) + \exp(-\alpha^2) \exp(-i\alpha^2) + \exp(-\alpha^2) \exp(-i\alpha^2) + \exp(-\alpha^2) \exp(i\alpha^2)] \\
 &= \frac{2(\alpha^2)^{4k} \exp(-\alpha^2)}{N_+} [\exp(i\alpha^2) + \exp(-i\alpha^2)] \\
 &= \frac{4(\alpha^2)^{4k} \exp(-\alpha^2)}{N_+} \cos(\alpha^2) \\
 &= \frac{4(\alpha^2)^{4k} \exp(-\alpha^2)}{4 \exp(-\alpha^2) \cosh(\alpha^2)} \cos(\alpha^2) = \frac{(\alpha^2)^{4k} \cos(\alpha^2)}{\cosh(\alpha^2)}, \tag{B1}
 \end{aligned}$$

$$\langle \bar{0}_+ | (\hat{a}^{4k})^\dagger \hat{a}^{4k} | \bar{0}_+ \rangle = \langle \bar{1}_+ | (\hat{a}^{4k})^\dagger \hat{a}^{4k} | \bar{1}_+ \rangle = (\alpha^2)^{4k}, \tag{B2}$$

$$\langle \bar{0}_+ | (\hat{a}^{4k})^\dagger \hat{a}^{4k+1} | \bar{0}_+ \rangle = \langle \bar{0}_+ | (\hat{a}^{4k})^\dagger \hat{a}^{4k+1} | \bar{1}_+ \rangle = \langle \bar{1}_+ | (\hat{a}^{4k})^\dagger \hat{a}^{4k+1} | \bar{1}_+ \rangle = \langle \bar{1}_+ | (\hat{a}^{4k})^\dagger \hat{a}^{4k+1} | \bar{0}_+ \rangle = 0, \tag{B3}$$

$$\begin{aligned}
 \langle \bar{0}_+ | (\hat{a}^{4k+1})^\dagger \hat{a}^{4k+1} | \bar{1}_+ \rangle &= \frac{1}{N_+} (\langle \alpha | + \langle -\alpha |) (\hat{a}^{4k+1})^\dagger \hat{a}^{4k+1} (|i\alpha\rangle + | -i\alpha\rangle) = \frac{i(\alpha^2)^{4k+1}}{N_+} (\langle \alpha | - \langle -\alpha |) (|i\alpha\rangle - | -i\alpha\rangle) \\
 &= \frac{i(\alpha^2)^{4k+1}}{N_+} [\exp(-\alpha^2) \exp(i\alpha^2) - \exp(-\alpha^2) \exp(-i\alpha^2) - \exp(-\alpha^2) \exp(-i\alpha^2) + \exp(-\alpha^2) \exp(i\alpha^2)] \\
 &= \frac{2i(\alpha^2)^{4k+1} \exp(-\alpha^2)}{N_+} [\exp(i\alpha^2) - \exp(-i\alpha^2)] = -\frac{4(\alpha^2)^{4k+1} \exp(-\alpha^2)}{N_+} \sin(\alpha^2) \\
 &= -\frac{(\alpha^2)^{4k+1} \sin(\alpha^2)}{\cosh(\alpha^2)}, \tag{B4}
 \end{aligned}$$

$$\langle \bar{0}_+ | (\hat{a}^{4k+1})^\dagger \hat{a}^{4k+1} | \bar{0}_+ \rangle = \langle \bar{1}_+ | (\hat{a}^{4k+1})^\dagger \hat{a}^{4k+1} | \bar{1}_+ \rangle = \frac{(\alpha^2)^{4k+1} N_-}{N_+}. \tag{B5}$$

Written in the Fock basis, the basic codewords read

$$\begin{aligned}
 |\bar{0}_+\rangle &= \frac{1}{\sqrt{\cosh(\alpha^2)}} \sum_{n=0}^{\infty} \frac{\alpha^{2n}}{\sqrt{(2n)!}} |2n\rangle, \\
 |\bar{1}_+\rangle &= \frac{1}{\sqrt{\cosh(\alpha^2)}} \sum_{n=0}^{\infty} \frac{(-1)^n \alpha^{2n}}{\sqrt{(2n)!}} |2n\rangle. \tag{B6}
 \end{aligned}$$

Like in the annihilation operator model, it is useful to study even and odd losses on the codewords separately:

$$\begin{aligned}
 A_{2m} |\bar{0}_+\rangle &= \frac{1}{\sqrt{\cosh(\alpha^2)}} \sum_{n=m}^{\infty} \frac{\alpha^{2n}}{\sqrt{(2n)!}} \sqrt{\gamma^{2n-2m}} \sqrt{1-\gamma}^{2m} \sqrt{\frac{(2n)!}{(2n-2m)!(2m)!}} |2n-2m\rangle \\
 &= \frac{1}{\sqrt{\cosh(\alpha^2)}} \sum_{n=m}^{\infty} \frac{\alpha^{2n}}{\sqrt{(2n-2m)!(2m)!}} \sqrt{\gamma^{2n-2m}} \sqrt{1-\gamma}^{2m} |2n-2m\rangle \\
 &= \frac{1}{\sqrt{(2m)!} \sqrt{\cosh(\alpha^2)}} \sqrt{1-\gamma}^{2m} \alpha^{2m} \sum_{l=0}^{\infty} \frac{\alpha^{2l}}{\sqrt{(2l)!}} \sqrt{\gamma^{2l}} |2l\rangle = \sqrt{\frac{\cosh(\alpha^2 \gamma)}{\cosh(\alpha^2)}} \frac{\sqrt{1-\gamma}^{2m} \alpha^{2m}}{\sqrt{(2m)!}} |\tilde{0}_+\rangle, \tag{B7}
 \end{aligned}$$

$$\begin{aligned}
A_{2m}|\bar{1}_+\rangle &= \frac{1}{\sqrt{\cosh(\alpha^2)}} \sum_{n=m}^{\infty} \frac{i^{2n}\alpha^{2n}}{\sqrt{(2n)!}} \sqrt{\gamma^{2n-2m}} \sqrt{1-\gamma}^{2m} \sqrt{\frac{(2n)!}{(2n-2m)!(2m)!}} |2n-2m\rangle \\
&= \frac{1}{\sqrt{\cosh(\alpha^2)}} \sum_{n=m}^{\infty} \frac{i^{2n}\alpha^{2n}}{\sqrt{(2n-2m)!(2m)!}} \sqrt{\gamma^{2n-2m}} \sqrt{1-\gamma}^{2m} |2n-2m\rangle \\
&= \frac{1}{\sqrt{(2m)!}\sqrt{\cosh(\alpha^2)}} \sqrt{1-\gamma}^{2m} \alpha^{2m} i^{2m} \sum_{l=0}^{\infty} (-1)^l \frac{\alpha^{2l}}{\sqrt{(2l)!}} \sqrt{\gamma^{2l}} |2l\rangle = \sqrt{\frac{\cosh(\alpha^2\gamma)}{\cosh(\alpha^2)}} \frac{\sqrt{1-\gamma}^{2m} \alpha^{2m} i^{2m}}{\sqrt{(2m)!}} |\tilde{1}_+\rangle, \quad (\text{B8})
\end{aligned}$$

$$\begin{aligned}
A_{2m+1}|\bar{0}_+\rangle &= \frac{1}{\sqrt{\cosh(\alpha^2)}} \sum_{n=m}^{\infty} \frac{\alpha^{2n}}{\sqrt{(2n)!}} \sqrt{\gamma^{2n-2m-1}} \sqrt{1-\gamma}^{2m+1} \sqrt{\frac{(2n)!}{(2n-2m-1)!(2m+1)!}} |2n-2m-1\rangle \\
&= \frac{1}{\sqrt{\cosh(\alpha^2)}} \sum_{n=m}^{\infty} \frac{\alpha^{2n}}{\sqrt{(2n-2m-1)!(2m+1)!}} \sqrt{\gamma^{2n-2m-1}} \sqrt{1-\gamma}^{2m+1} |2n-2m-1\rangle \\
&= \frac{1}{\sqrt{(2m)!}\sqrt{\cosh(\alpha^2)}} \sqrt{1-\gamma}^{2m+1} \alpha^{2m+1} \sum_{l=0}^{\infty} \frac{\alpha^{2l+1}}{\sqrt{(2l+1)!}} \sqrt{\gamma^{2l+1}} |2l+1\rangle = \sqrt{\frac{\sinh(\alpha^2\gamma)}{\cosh(\alpha^2)}} \frac{\sqrt{1-\gamma}^{2m+1} \alpha^{2m+1}}{\sqrt{(2m+1)!}} |\tilde{0}_-\rangle, \quad (\text{B9})
\end{aligned}$$

$$\begin{aligned}
A_{2m+1}|\bar{1}_+\rangle &= \frac{1}{\sqrt{\cosh(\alpha^2)}} \sum_{n=m}^{\infty} \frac{i^{2n}\alpha^{2n}}{\sqrt{(2n)!}} \sqrt{\gamma^{2n-2m-1}} \sqrt{1-\gamma}^{2m+1} \sqrt{\frac{(2n)!}{(2n-2m-1)!(2m+1)!}} |2n-2m-1\rangle \\
&= \frac{1}{\sqrt{\cosh(\alpha^2)}} \sum_{n=m}^{\infty} \frac{i^{2n}\alpha^{2n}}{\sqrt{(2n-2m-1)!(2m+1)!}} \sqrt{\gamma^{2n-2m-1}} \sqrt{1-\gamma}^{2m+1} |2n-2m-1\rangle \\
&= \frac{1}{\sqrt{(2m)!}\sqrt{\cosh(\alpha^2)}} \sqrt{1-\gamma}^{2m+1} \alpha^{2m+1} i^{2m+1} \sum_{l=0}^{\infty} (-1)^l \frac{\alpha^{2l+1}}{\sqrt{(2l+1)!}} \sqrt{\gamma^{2l}} |2l+1\rangle \\
&= \sqrt{\frac{\sinh(\alpha^2\gamma)}{\cosh(\alpha^2)}} \frac{\sqrt{1-\gamma}^{2m+1} \alpha^{2m+1} i^{2m+1}}{\sqrt{(2m+1)!}} |\tilde{1}_-\rangle. \quad (\text{B10})
\end{aligned}$$

One can easily verify that the norms of corrupted codewords are identical; i.e., the logical qubits are not deformed after loss. Qualitatively, we find the same cyclic behavior as in the simplified loss model. Note, however, that the logical codewords in the different error spaces are not orthogonal for finite α . The encoding presented here is therefore not an exact QEC code but can be regarded as an approximate QEC code, provided α is taken sufficiently large to ensure near orthogonality.

From the expressions above, the probabilities for individual losses on the codewords can easily be determined by calculating the corresponding squared norm:

$$\begin{aligned}
p_0 &= \frac{\cosh(\alpha^2\gamma)}{\cosh(\alpha^2)} \sum_{m=0,2,4,\dots}^{\infty} \frac{[(1-\gamma)\alpha^2]^{2m}}{(2m)!} = \frac{\cosh(\gamma\alpha^2)}{2\cosh(\alpha^2)} \{\cos[\alpha^2(1-\gamma)] + \cosh[\alpha^2(1-\gamma)]\}, \\
p_1 &= \frac{\sinh(\alpha^2\gamma)}{\cosh(\alpha^2)} \sum_{m=0,2,4,\dots}^{\infty} \frac{[(1-\gamma)\alpha^2]^{2m+1}}{(2m+1)!} = \frac{\sinh(\gamma\alpha^2)}{2\cosh(\alpha^2)} \{\sin[\alpha^2(1-\gamma)] + \sinh[\alpha^2(1-\gamma)]\}, \\
p_2 &= \frac{\cosh(\alpha^2\gamma)}{\cosh(\alpha^2)} \sum_{m=1,3,5,\dots}^{\infty} \frac{[(1-\gamma)\alpha^2]^{2m}}{(2m)!} = \frac{\cosh(\gamma\alpha^2)}{2\cosh(\alpha^2)} \{-\cos[\alpha^2(1-\gamma)] + \cosh[\alpha^2(1-\gamma)]\}, \\
p_3 &= \frac{\sinh(\alpha^2\gamma)}{\cosh(\alpha^2)} \sum_{m=1,3,5,\dots}^{\infty} \frac{[(1-\gamma)\alpha^2]^{2m+1}}{(2m+1)!} = \frac{\sinh(\gamma\alpha^2)}{2\cosh(\alpha^2)} \{-\sin[\alpha^2(1-\gamma)] + \sinh[\alpha^2(1-\gamma)]\}. \quad (\text{B11})
\end{aligned}$$

Note that p_0 contains the probability for no loss, four losses, eight losses and so on.

We are interested in the evolution of a logical qubit subject to photon loss. Taking the finite overlap of the codewords into account, a properly normalized qubit reads as

$$|\bar{\psi}\rangle = \frac{a|\bar{0}_+\rangle + b|\bar{1}_+\rangle}{\sqrt{1 + 2\operatorname{Re}(ab^*)\langle\bar{0}_+|\bar{1}_+\rangle}}. \quad (\text{B12})$$

The codewords are not deformed, such that after a loss, say one loss and the cyclic equivalents, a global factor p_1 arises. In addition to that, we have to take the nonorthogonality of the codewords in the error spaces into account; i.e. we have to properly renormalize the erroneous state. In this example, we get a relative phase of i which changes the norm of the qubit as well as the damped amplitude:

$$A_1|\tilde{\psi}\rangle = \sqrt{\frac{1 - 2 \operatorname{Re}(a^*b) \frac{\sin(\gamma\alpha^2)}{\sinh(\gamma\alpha^2)}}{1 + 2 \operatorname{Re}(ab^*) \frac{\cos(\alpha^2)}{\cosh(\alpha^2)}}} p_1 \times \left[\frac{a|\tilde{0}_-\rangle + ib|\tilde{1}_-\rangle}{\sqrt{1 - 2 \operatorname{Re}(a^*b) \frac{\sin(\gamma\alpha^2)}{\sinh(\gamma\alpha^2)}}} \right]. \quad (\text{B13})$$

The loss probability is therefore

$$\tilde{p}_1 = \frac{1 - 2 \operatorname{Re}(a^*b) \frac{\sin(\gamma\alpha^2)}{\sinh(\gamma\alpha^2)}}{1 + 2 \operatorname{Re}(ab^*) \frac{\cos(\alpha^2)}{\cosh(\alpha^2)}} p_1, \quad (\text{B14})$$

and the normalized state reads

$$\left[\frac{a|\tilde{0}_-\rangle + ib|\tilde{1}_-\rangle}{\sqrt{1 - 2 \operatorname{Re}(a^*b) \frac{\sin(\gamma\alpha^2)}{\sinh(\gamma\alpha^2)}}} \right]. \quad (\text{B15})$$

The analogous results for the loss probabilities and the total final mixed states are summarised in the main text.

For comparison, let us investigate the KL conditions for the codewords in the \tilde{X} basis [see also the discussion after Eq. (4) in the main text]:

$$\begin{aligned} |\tilde{0}_+ + \tilde{1}_+\rangle &= \frac{1}{\sqrt{N'_+}} (|\tilde{0}_+\rangle + |\tilde{1}_+\rangle), \\ |\tilde{0}_+ - \tilde{1}_+\rangle &= \frac{1}{\sqrt{N'_-}} (|\tilde{0}_+\rangle - |\tilde{1}_+\rangle). \end{aligned} \quad (\text{B16})$$

We consider again the error set $\mathcal{E} = \{\hat{a}^{4k}, \hat{a}^{4k+1}, k \in \mathbb{N}_0\}$. The action on the \tilde{X} -basis codewords can be easily calculated based on the results of the \tilde{Z} -basis analysis:

$$\begin{aligned} \hat{a}^{4k}|\tilde{0}_+ + \tilde{1}_+\rangle &= \alpha^{4k}|\tilde{0}_+ + \tilde{1}_+\rangle = \frac{\alpha^{4k}}{\sqrt{N'_+}} (|\tilde{0}_+\rangle + |\tilde{1}_+\rangle), \\ \hat{a}^{4k}|\tilde{0}_+ - \tilde{1}_+\rangle &= \alpha^{4k}|\tilde{0}_+ - \tilde{1}_+\rangle = \frac{\alpha^{4k}}{\sqrt{N'_-}} (|\tilde{0}_+\rangle - |\tilde{1}_+\rangle), \\ \hat{a}^{4k+1}|\tilde{0}_+ + \tilde{1}_+\rangle &= \frac{\alpha^{4k+1}}{\sqrt{N'_+}} (|\tilde{0}_-\rangle + i|\tilde{1}_-\rangle), \\ \hat{a}^{4k+1}|\tilde{0}_+ - \tilde{1}_+\rangle &= \frac{\alpha^{4k+1}}{\sqrt{N'_-}} (|\tilde{0}_-\rangle - i|\tilde{1}_-\rangle). \end{aligned} \quad (\text{B17})$$

The orthogonality requirements are fulfilled as

$$\begin{aligned} \langle \tilde{0}_+ + \tilde{1}_+ | (\hat{a}^{4k})^\dagger \hat{a}^{4k} | \tilde{0}_+ - \tilde{1}_+ \rangle &= \langle \tilde{0}_+ + \tilde{1}_+ | (\hat{a}^{4k+1})^\dagger \hat{a}^{4k+1} | \tilde{0}_+ - \tilde{1}_+ \rangle \\ &= \langle \tilde{0}_+ + \tilde{1}_+ | (\hat{a}^{4k+1})^\dagger \hat{a}^{4k} | \tilde{0}_+ - \tilde{1}_+ \rangle \\ &= \langle \tilde{0}_+ - \tilde{1}_+ | (\hat{a}^{4k+1})^\dagger \hat{a}^{4k} | \tilde{0}_+ + \tilde{1}_+ \rangle. \end{aligned} \quad (\text{B18})$$

The nondeformation criterion for \hat{a}^{4k} reads

$$\begin{aligned} \langle \tilde{0}_+ + \tilde{1}_+ | (\hat{a}^{4k})^\dagger \hat{a}^{4k} | \tilde{0}_+ - \tilde{1}_+ \rangle &= \langle \tilde{0}_+ - \tilde{1}_+ | (\hat{a}^{4k})^\dagger \hat{a}^{4k} | \tilde{0}_+ - \tilde{1}_+ \rangle \\ &= (\alpha^2)^{4k}. \end{aligned} \quad (\text{B19})$$

However, for \hat{a}^{4k+1} we have

$$\begin{aligned} \langle \tilde{0}_+ + \tilde{1}_+ | (\hat{a}^{4k+1})^\dagger \hat{a}^{4k+1} | \tilde{0}_+ + \tilde{1}_+ \rangle &= \frac{2(\alpha^2)^{4k+1}}{N'_+} \left[1 - \frac{\sin(\alpha^2)}{\sinh(\alpha^2)} \right], \\ \langle \tilde{0}_+ - \tilde{1}_+ | (\hat{a}^{4k+1})^\dagger \hat{a}^{4k+1} | \tilde{0}_+ - \tilde{1}_+ \rangle &= \frac{2(\alpha^2)^{4k+1}}{N'_-} \left[1 + \frac{\sin(\alpha^2)}{\sinh(\alpha^2)} \right], \end{aligned} \quad (\text{B20})$$

which shows a violation of the nondeformation criterion. This can only be overcome with sufficiently large α .

APPENDIX C: ERROR-CORRECTION STEPS AND LOWER BOUND ON FIDELITY

We discuss the error-correction procedure and the fidelity as a figure of merit for the example of the one-loss cat code. An extension to the higher-loss codes is straightforward.

The first step for correcting loss-induced errors on an incoming logical qubit is to determine its photon-number parity (even or odd) and hence the subspace in which the qubit resides (code or error space). After this first error-correction step, i.e., the number parity measurement that projects $\tilde{\rho}$ either onto the even space with the normalized conditional density matrix

$$\begin{aligned} \rho^{(+)} &= \frac{1}{P^+} \left\{ \tilde{p}_0 \left[\frac{a|\tilde{0}_+\rangle + b|\tilde{1}_+\rangle}{\sqrt{1 + 2 \operatorname{Re}(ab^*) \frac{\cos(\gamma\alpha^2)}{\cosh(\gamma\alpha^2)}}} \right] \times \text{H.c.} \right. \\ &\quad \left. + \tilde{p}_2 \left[\frac{a|\tilde{0}_+\rangle - b|\tilde{1}_+\rangle}{\sqrt{1 - 2 \operatorname{Re}(ab^*) \frac{\cos(\gamma\alpha^2)}{\cosh(\gamma\alpha^2)}}} \right] \times \text{H.c.} \right\} \quad (\text{C1}) \end{aligned}$$

or onto the odd space with the corresponding density matrix

$$\begin{aligned} \rho^{(-)} &= \frac{1}{P^-} \left\{ \tilde{p}_1 \left[\frac{a|\tilde{0}_-\rangle + ib|\tilde{1}_-\rangle}{\sqrt{1 - 2 \operatorname{Re}(ab^*) \frac{\sin(\gamma\alpha^2)}{\sinh(\gamma\alpha^2)}}} \right] \times \text{H.c.} \right. \\ &\quad \left. + \tilde{p}_3 \left[\frac{a|\tilde{0}_-\rangle - ib|\tilde{1}_-\rangle}{\sqrt{1 + 2 \operatorname{Re}(ab^*) \frac{\sin(\gamma\alpha^2)}{\sinh(\gamma\alpha^2)}}} \right] \times \text{H.c.} \right\}, \quad (\text{C2}) \end{aligned}$$

as a second step, the amplitudes are probabilistically restored, $|\tilde{0}_+\rangle \rightarrow |\tilde{0}_+\rangle$, etc., while the odd states are also teleported back into the even space (see Appendix F). Here P^+ and P^- are the probabilities for obtaining the error syndromes ‘‘even’’ (code space) and ‘‘odd’’ (error space), respectively (they correspond to the trace of the respective expression in squared brackets, i.e., each unnormalized conditional state). The worst-case

fidelity is defined as

$$F_{wc} = \min_{a,b} [\langle \tilde{\psi} | \hat{\rho}^{(+)} | \tilde{\psi} \rangle P^+ + \langle \tilde{\psi}' | \hat{\rho}^{(-)} | \tilde{\psi}' \rangle P^-] = \min_{a,b} \left\{ \tilde{p}_0(a,b) + \tilde{p}_2(a,b) \left| \langle \tilde{\psi} | \left[\frac{a|\bar{0}_+\rangle - b|\bar{1}_+\rangle}{\sqrt{1 - 2 \operatorname{Re}(ab^*) \frac{\cosh(\alpha^2)}{\cosh(\alpha^2)}}} \right] \right|^2 \right. \\ \left. + \tilde{p}_1(a,b) + \tilde{p}_3(a,b) \left| \langle \tilde{\psi}' | \left[\frac{a|\bar{0}_+\rangle - ib|\bar{1}_+\rangle}{\sqrt{1 - 2 \operatorname{Re}(iab^*) \frac{\cosh(\alpha^2)}{\cosh(\alpha^2)}}} \right] \right|^2 \right\}, \quad (\text{C3})$$

where $|\tilde{\psi}'\rangle = \frac{a|\bar{0}_+\rangle + ib|\bar{1}_+\rangle}{\sqrt{1 - 2 \operatorname{Re}(iab^*) \frac{\cosh(\alpha^2)}{\cosh(\alpha^2)}}}$ (i.e., the reference input state for the odd syndrome has a fixed phase gate applied to it compared to the original qubit input state $|\tilde{\psi}\rangle = \frac{a|\bar{0}_+\rangle + b|\bar{1}_+\rangle}{\sqrt{1 + 2 \operatorname{Re}(ab^*) \frac{\cosh(\alpha^2)}{\cosh(\alpha^2)}}}$).

The second term in each of the last two lines of Eq. (C3) is non-negative. If both terms vanish (i.e., we have $\alpha \rightarrow \infty$ and $a = \frac{1}{\sqrt{2}} = \pm b$), \tilde{p}_0 and \tilde{p}_1 no longer depend on a and b , and $F_{wc} = \tilde{p}_0 + \tilde{p}_1$ [more generally: $F_{wc} = \tilde{p}_0(a^{wc}, b^{wc}) + \tilde{p}_1(a^{wc}, b^{wc}) \geq \min_{a,b} (\tilde{p}_0 + \tilde{p}_1)$].

For the other case when the two relevant terms in Eq. (C3) do not vanish, we have

$$F_{wc} > \tilde{p}_0(a^{wc}, b^{wc}) + \tilde{p}_1(a^{wc}, b^{wc}) \geq \min_{a,b} (\tilde{p}_0 + \tilde{p}_1). \quad (\text{C4})$$

Thus, in general, we obtain the bound on F_{wc} as expressed by Eq. (17).

We show in the following that the probability for correct syndrome identification $F(a,b)$ for $L = 1$ and a logical qubit $a|\bar{0}_+\rangle + b|\bar{1}_+\rangle$ under the conditions $a, b \in \mathbb{R}$ is extremal for $|a| = |b| = \frac{1}{\sqrt{2}}$.

The fidelity can be cast in the following form:

$$F(a,b) = \frac{1 + 2abc_1}{1 + 2abc_2} p_0 + \frac{1 - 2abc_3}{1 + 2abc_2} p_1 \\ = \frac{1 + 2a\sqrt{1 - a^2}c_1}{1 + 2a\sqrt{1 - a^2}c_2} p_0 + \frac{1 - 2a\sqrt{1 - a^2}c_3}{1 + 2a\sqrt{1 - a^2}c_2} p_1 \\ = \frac{p_0 + p_1 + 2a\sqrt{1 - a^2}(c_1 p_0 - c_3 p_1)}{1 + 2a\sqrt{1 - a^2}c_2} \\ = F(a). \quad (\text{C5})$$

Here the coefficients are shorthand for the overlaps of the codewords in the different error spaces; see Eqs. (13)–(15) and Eqs. (3) and (10). These coefficients are real and bounded by 1. To find the extremal value of the fidelity, we derive F with respect to a :

$$\frac{dF}{da} = \frac{(1 + 2a\sqrt{1 - a^2}c_2)(c_1 p_0 - c_3 p_1) \frac{2-4a^2}{\sqrt{1-a^2}}}{(1 + 2a\sqrt{1 - a^2}c_2)^2} \\ - \frac{[p_0 + p_1 + 2a\sqrt{1 - a^2}(c_1 p_0 - c_3 p_1)]c_2 \frac{2-4a^2}{\sqrt{1-a^2}}}{(1 + 2a\sqrt{1 - a^2}c_2)^2} \\ \propto 2 - 4a^2. \quad (\text{C6})$$

This vanishes for $a^2 = \frac{1}{2}$ and therefore we find the two solutions $a = \pm \frac{1}{\sqrt{2}}$. One solution corresponds to a maximum and the other to a minimum. The second derivative can resolve this and the solution depends on the signs of the coefficients c_i .

To be safe and to avoid complicated formulas, one can clearly set

$$f_{\min}(a) := \min \left\{ F\left(a = \frac{1}{\sqrt{2}}\right), F\left(a = -\frac{1}{\sqrt{2}}\right) \right\}, \quad (\text{C7})$$

which then corresponds to the lower bound F on the worst-case fidelity F_{wc} , as shown in Eq. (17).

APPENDIX D: DERIVATION OF CODEWORDS IN THE FOCK BASIS

To solve the system of equations (18), we set $|\bar{0}\rangle = \sum_{n=0}^{\infty} c_n |n\rangle$. We have

$$\hat{a}^{L+1} |\bar{0}\rangle = \sum_{n=L+1}^{\infty} c_n \sqrt{n} \sqrt{n-1} \cdots \sqrt{n-L} |n-L-1\rangle \\ = \sum_{k=0}^{\infty} c_{k+L+1} \sqrt{k+L+1} \sqrt{k+L} \cdots \sqrt{k+1} |k\rangle \\ = \alpha^{L+1} \sum_{k=0}^{\infty} c_k |k\rangle. \quad (\text{D1})$$

One obtains a recursive definition of the coefficients:

$$c_{k+L+1} = \frac{\alpha^{L+1} c_k}{\sqrt{k+L+1} \sqrt{k+L} \cdots \sqrt{k+1}}. \quad (\text{D2})$$

To solve the series, one of the first parameters, c_0 or c_1 , has to be fixed.

Before determining the general solution, let us examine the easiest example, $L = 0$. Here the parity condition is trivial and the other two equations are just the defining equations for coherent states. Therefore, the system of equations leads to $|\bar{0}\rangle = |\alpha\rangle$ and $|\bar{1}\rangle = |-\alpha\rangle$.

As another illustrative example, we choose $L = 1$. Then we find the series:

$$c_{k+2} = \frac{\alpha^2 c_k}{\sqrt{k+2} \sqrt{k+1}}. \quad (\text{D3})$$

If we set c_0 as given, this series is resolved by

$$c_{2k} = \frac{\alpha^{2k} c_0}{\sqrt{(2k)!}}. \quad (\text{D4})$$

However, c_0 is not arbitrary, because it follows from the normalization constraint

$$\sum_{k=0}^{\infty} |c_{2k}|^2 = \sum_{k=0}^{\infty} \frac{(\alpha^2)^{2k}}{(2k)!} |c_0|^2 = 1 \Rightarrow |c_0|. \quad (\text{D5})$$

The coefficient c_0 is then determined up to a irrelevant phase which leads to a global phase because of (D4). The corresponding recursion formula for $|\bar{1}\rangle$ is given by

$$c_{2k} = \frac{(-1)^k \alpha^{2k} c_0}{\sqrt{(2k)!}}, \quad (\text{D6})$$

where c_0 can be determined through normalization. Therefore, in the Fock basis, the basis codewords read

$$\begin{aligned} |\bar{0}\rangle &= \frac{1}{\sqrt{\cosh(\alpha^2)}} \sum_{n=0}^{\infty} \frac{\alpha^{2n}}{\sqrt{(2n)!}} |2n\rangle, \\ |\bar{1}\rangle &= \frac{1}{\sqrt{\cosh(\alpha^2)}} \sum_{n=0}^{\infty} (-1)^n \frac{\alpha^{2n}}{\sqrt{(2n)!}} |2n\rangle. \end{aligned} \quad (\text{D7})$$

This can be expressed in terms of coherent states

$$\begin{aligned} |\bar{0}\rangle &= \frac{1}{\sqrt{N_+}} (|\alpha\rangle + |-\alpha\rangle), \\ |\bar{1}\rangle &= \frac{1}{\sqrt{N_+}} (i|\alpha\rangle + |-i\alpha\rangle), \end{aligned} \quad (\text{D8})$$

as given in Sec. II.

If we fix c_1 , a completely analogous calculation leads to

$$\begin{aligned} |\bar{0}\rangle &= \frac{1}{\sqrt{\sinh(\alpha^2)}} \sum_{n=0}^{\infty} \frac{\alpha^{2n+1}}{\sqrt{(2n+1)!}} |2n+1\rangle, \\ |\bar{1}\rangle &= \frac{1}{\sqrt{\sinh(\alpha^2)}} \sum_{n=0}^{\infty} (-1)^n \frac{\alpha^{2n+1}}{\sqrt{(2n+1)!}} |2n+1\rangle. \end{aligned} \quad (\text{D9})$$

Since the parity condition for $L = 1$ reads as $(-1)^{\hat{n}} |\bar{\psi}\rangle = |\bar{\psi}\rangle$, the first pair of codewords is the solution of the determining system of equations.

For general L , it is easy to verify that the (unnormalized) solutions of the defining equations in the Fock basis are given by

$$\begin{aligned} |\bar{0}\rangle &= \sum_{k=0}^{\infty} \frac{\alpha^{(L+1)k}}{\sqrt{[(L+1)k]!}} |(L+1)k\rangle, \\ |\bar{1}\rangle &= \sum_{k=0}^{\infty} \frac{(-1)^k \alpha^{(L+1)k}}{\sqrt{[(L+1)k]!}} |(L+1)k\rangle. \end{aligned} \quad (\text{D10})$$

We show in the following these states can be rewritten in terms of coherent states as presented in the main text:

$$\begin{aligned} |\bar{0}\rangle &= \sum_{k=0}^L \left| \alpha \exp\left(\frac{2\pi i k}{L+1}\right) \right\rangle, \\ |\bar{1}\rangle &= \sum_{k=1}^{L+1} \left| \alpha \exp\left[\frac{(2k-1)\pi i}{L+1}\right] \right\rangle. \end{aligned} \quad (\text{D11})$$

Expressed in the Fock basis, we have

$$\begin{aligned} |\bar{0}\rangle &= \sum_{k=0}^L \sum_{r=0}^{\infty} \frac{\alpha^r \exp\left(\frac{\pi i 2k}{L+1}\right)^r}{\sqrt{r!}} |r\rangle \\ &= \sum_{r=0}^{\infty} \frac{\alpha^r}{\sqrt{r!}} |r\rangle \sum_{k=0}^L \exp\left(\frac{\pi i 2r}{L+1}\right)^k \\ &= \sum_{r=0}^{\infty} \frac{\alpha^r}{\sqrt{r!}} |r\rangle \frac{1 - \exp(\pi i 2r)}{1 - \exp\left(\frac{\pi i 2r}{L+1}\right)} \end{aligned}$$

$$\begin{aligned} &= \sum_{r,m=0}^{\infty} \frac{\alpha^r}{\sqrt{r!}} |r\rangle \delta_r^{(L+1)m} \\ &= \sum_{m=0}^{\infty} \frac{\alpha^{(L+1)m}}{\sqrt{[(L+1)m]!}} |(L+1)m\rangle. \end{aligned} \quad (\text{D12})$$

The calculation for the other codeword is similar,

$$\begin{aligned} |\bar{1}\rangle &= \sum_{k=1}^{L+1} \sum_{r=0}^{\infty} \frac{\alpha^r \exp\left[\frac{\pi i (2k-1)}{L+1}\right]^r}{\sqrt{r!}} |r\rangle \\ &= \sum_{r=0}^{\infty} \frac{\alpha^r}{\sqrt{r!}} |r\rangle \sum_{k=1}^{L+1} \exp\left(\frac{\pi i r}{L+1}\right)^{2k-1} \\ &= \sum_{r=0}^{\infty} \frac{\alpha^r}{\sqrt{r!}} |r\rangle \exp\left(-\frac{\pi i r}{L+1}\right) \sum_{k=1}^{L+1} \exp\left(\frac{2\pi i r}{L+1}\right)^k \\ &= \sum_{r=0}^{\infty} \frac{\alpha^r}{\sqrt{r!}} |r\rangle \exp\left(\frac{\pi i r}{L+1}\right) \sum_{j=0}^L \exp\left(\frac{2\pi i r}{L+1}\right)^j \\ &= \sum_{r=0}^{\infty} \frac{\alpha^r}{\sqrt{r!}} |r\rangle \exp\left(\frac{\pi i r}{L+1}\right) \frac{1 - \exp(\pi i 2r)}{1 - \exp\left(\frac{\pi i 2r}{L+1}\right)} \\ &= \sum_{r,m=0}^{\infty} \frac{\alpha^r}{\sqrt{r!}} |r\rangle \exp\left(\frac{\pi i r}{L+1}\right) \delta_r^{(L+1)m} \\ &= \sum_{m=0}^{\infty} \frac{(-1)^m \alpha^{(L+1)m}}{\sqrt{[(L+1)m]!}} |(L+1)m\rangle. \end{aligned} \quad (\text{D13})$$

Up to normalization, the basic codewords in the $L+1$ error spaces in terms of coherent states are defined as

$$\begin{aligned} |\bar{0}_q\rangle_L &:= \sum_{k=0}^L \exp\left(\frac{2qki\pi}{L+1}\right) \left| \alpha \exp\left(\frac{2ki\pi}{L+1}\right) \right\rangle, \\ |\bar{1}_q\rangle_L &:= \sum_{k=1}^{L+1} \exp\left[\frac{2q(k-1)i\pi}{L+1}\right] \left| \alpha \exp\left[\frac{(2k-1)i\pi}{L+1}\right] \right\rangle \end{aligned} \quad (\text{D14})$$

for $q = 0, \dots, L$. In the Fock basis, these can be expressed as

$$\begin{aligned} |\bar{0}_q\rangle_L &:= \sum_{k=1}^{\infty} \frac{\alpha^{(L+1)k-q}}{\sqrt{[(L+1)k-q]!}} |(L+1)k-q\rangle, \\ |\bar{1}_q\rangle_L &:= \sum_{k=1}^{\infty} \frac{(e^{\frac{i\pi}{L+1}} \alpha)^{(L+1)k-q}}{\sqrt{[(L+1)k-q]!}} |(L+1)k-q\rangle. \end{aligned} \quad (\text{D15})$$

The code-defining equations, including both the code space and all error spaces, then become

$$\begin{aligned} \exp\left(\frac{2\pi i \hat{n}}{L+1}\right) |\bar{0}_q\rangle_L &= \exp\left(\frac{2\pi i q}{L+1}\right) |\bar{0}_q\rangle_L, \\ \exp\left(\frac{2\pi i \hat{n}}{L+1}\right) |\bar{1}_q\rangle_L &= \exp\left(\frac{2\pi i q}{L+1}\right) |\bar{1}_q\rangle_L, \\ (\hat{a}^{L+1} - \alpha^{L+1}) |\bar{0}_q\rangle_L &= 0, \\ (\hat{a}^{L+1} + \alpha^{L+1}) |\bar{1}_q\rangle_L &= 0, \end{aligned} \quad (\text{D16})$$

$\forall q = 0, 1, 2, \dots, L$. The evolution of a logical qubit $|\bar{\Psi}\rangle = \frac{a|\bar{0}\rangle + b|\bar{1}\rangle}{\sqrt{1 + 2\operatorname{Re}(ab^*(\bar{0}|\bar{1})}}}$ under AD can then be described as an (unnormalized) mixture of $2(L + 1)$ components (we omit the code-defining subscript L outside the ket vectors):

$$\begin{aligned} \bar{\rho} = & p_0(a|\bar{0}_0\rangle + b|\bar{1}_0\rangle) \times \text{H.c.} + p_1(a|\bar{0}_1\rangle + e^{\frac{i\pi}{L+1}}b|\bar{1}_1\rangle) \times \text{H.c.} + p_2(a|\bar{0}_2\rangle + e^{\frac{2i\pi}{L+1}}b|\bar{1}_2\rangle) \times \text{H.c.} \\ & + p_3(a|\bar{0}_3\rangle + e^{\frac{3i\pi}{L+1}}b|\bar{1}_3\rangle) \times \text{H.c.} + \dots + p_L(a|\bar{0}_L\rangle + e^{\frac{Li\pi}{L+1}}b|\bar{1}_L\rangle) \times \text{H.c.} \\ & + p_{L+1}(a|\bar{0}_0\rangle - b|\bar{1}_0\rangle) \times \text{H.c.} + p_{L+2}(a|\bar{0}_1\rangle - e^{\frac{i\pi}{L+1}}b|\bar{1}_1\rangle) \times \text{H.c.} \\ & + p_{L+3}(a|\bar{0}_2\rangle - e^{\frac{2i\pi}{L+1}}b|\bar{1}_2\rangle) \times \text{H.c.} + \dots + p_{2L+1}(a|\bar{0}_L\rangle - e^{\frac{Li\pi}{L+1}}b|\bar{1}_L\rangle) \times \text{H.c.} \end{aligned} \quad (\text{D17})$$

APPENDIX E: FULL LOSS CHANNEL AND KL CONDITIONS FOR THE TWO-LOSS CODE

The normalized $L = 2$ codewords read in the Fock basis as

$$|\bar{0}\rangle = \frac{1}{\sqrt{N}} \sum_{k=0}^{\infty} \frac{\alpha^{3k}}{\sqrt{(3k)!}} |3k\rangle, \quad |\bar{1}\rangle = \frac{1}{\sqrt{N}} \sum_{k=0}^{\infty} \frac{(-\alpha)^{3k}}{\sqrt{(3k)!}} |3k\rangle, \quad (\text{E1})$$

where $N = \frac{1}{3}[\exp(\alpha^2) + 2\exp(-\frac{\alpha^2}{2})\cos(\frac{\sqrt{3}\alpha^2}{2})]$. The code-word overlap is given by

$$\langle \bar{1} | \bar{0} \rangle = \frac{\exp(-\alpha^2) + 2\exp(\frac{\alpha^2}{2})\cos(\frac{\sqrt{3}\alpha^2}{2})}{\exp(\alpha^2) + 2\exp(-\frac{\alpha^2}{2})\cos(\frac{\sqrt{3}\alpha^2}{2})} \xrightarrow{\alpha \rightarrow \infty} 0. \quad (\text{E2})$$

Based on the results obtained in Sec. III for the simplified error model, we expect a similar cyclic behavior of the code under the full AD channel. It is therefore advantageous to consider the action of the operators $\{A_{3k}, A_{3k+1}, A_{3k+2}\}$ on the codewords:

$$\begin{aligned} A_{3k}|\bar{0}\rangle &= \frac{1}{\sqrt{N}} \frac{\sqrt{1-\gamma}^{3k} \alpha^{3k}}{\sqrt{(3k)!}} \sum_{n=0}^{\infty} \frac{(\alpha\sqrt{\gamma})^{3n}}{\sqrt{(3n)!}} |3n\rangle, \\ A_{3k}|\bar{1}\rangle &= \frac{(-1)^k}{\sqrt{N}} \frac{\sqrt{1-\gamma}^{3k} \alpha^{3k}}{\sqrt{(3k)!}} \sum_{n=0}^{\infty} \frac{(-\alpha\sqrt{\gamma})^{3n}}{\sqrt{(3n)!}} |3n\rangle, \\ A_{3k+1}|\bar{0}\rangle &= \frac{1}{\sqrt{N}} \frac{\sqrt{1-\gamma}^{3k+1} \alpha^{3k+1}}{\sqrt{(3k+1)!}} \sum_{n=1}^{\infty} \frac{(\alpha\sqrt{\gamma})^{3n-1}}{\sqrt{(3n-1)!}} |3n-1\rangle, \\ A_{3k+1}|\bar{1}\rangle &= \frac{(-1)^{k+1}}{\sqrt{N}} \frac{\sqrt{1-\gamma}^{3k+1} \alpha^{3k+1} e^{\frac{\pi i}{3}}}{\sqrt{(3k+1)!}} \sum_{n=1}^{\infty} \frac{(e^{\frac{\pi i}{3}} \alpha\sqrt{\gamma})^{3n-1}}{\sqrt{(3n-1)!}} |3n-1\rangle, \\ A_{3k+2}|\bar{0}\rangle &= \frac{1}{\sqrt{N}} \frac{\sqrt{1-\gamma}^{3k+2} \alpha^{3k+2}}{\sqrt{(3k+2)!}} \sum_{n=1}^{\infty} \frac{(\alpha\sqrt{\gamma})^{3n-2}}{\sqrt{(3n-2)!}} |3n-2\rangle, \\ A_{3k+2}|\bar{1}\rangle &= \frac{(-1)^k}{\sqrt{N}} \frac{\sqrt{1-\gamma}^{3k+2} \alpha^{3k+2} e^{\frac{2\pi i}{3}}}{\sqrt{(3k+2)!}} \sum_{n=1}^{\infty} \frac{(e^{\frac{2\pi i}{3}} \alpha\sqrt{\gamma})^{3n-2}}{\sqrt{(3n-2)!}} |3n-2\rangle. \end{aligned} \quad (\text{E3})$$

Following the notation introduced after Eq. (22), the basic codewords in the three orthogonal error spaces read

$$\begin{aligned} |\tilde{0}_0\rangle_2 &\propto \sum_{k=0}^{\infty} \frac{(\alpha\sqrt{\gamma})^{3k}}{\sqrt{(3k)!}} |3k\rangle, \quad |\tilde{1}_0\rangle_2 \propto \sum_{k=0}^{\infty} \frac{(-\alpha\sqrt{\gamma})^{3k}}{\sqrt{(3k)!}} |3k\rangle, \quad |\tilde{0}_1\rangle_2 \propto \sum_{k=1}^{\infty} \frac{(\alpha\sqrt{\gamma})^{3k-1}}{\sqrt{(3k-1)!}} |3k-1\rangle, \\ |\tilde{1}_1\rangle_2 &\propto \sum_{k=1}^{\infty} \frac{(e^{\frac{\pi i}{3}} \alpha\sqrt{\gamma})^{3k-1}}{\sqrt{(3k-1)!}} |3k-1\rangle, \quad |\tilde{0}_2\rangle_2 \propto \sum_{k=1}^{\infty} \frac{(\alpha\sqrt{\gamma})^{3k-2}}{\sqrt{(3k-2)!}} |3k-2\rangle, \quad |\tilde{1}_2\rangle_2 \propto \sum_{k=1}^{\infty} \frac{(e^{\frac{2\pi i}{3}} \alpha\sqrt{\gamma})^{3k-2}}{\sqrt{(3k-2)!}} |3k-2\rangle, \end{aligned} \quad (\text{E4})$$

where \sim again indicates the damped amplitude. Obviously, the different error spaces are orthogonal and the codewords in each error space become orthogonal for large α .

Furthermore, we define the following logical states (\sim denotes again damped logical states):

$$\begin{aligned} |\tilde{\Psi}_0\rangle &\propto a|\tilde{0}_0\rangle_2 + b|\tilde{1}_0\rangle_2, \quad |\tilde{\Psi}_1\rangle \propto a|\tilde{0}_1\rangle_2 + e^{\frac{\pi i}{3}}b|\tilde{1}_1\rangle_2, \quad |\tilde{\Psi}_2\rangle \propto a|\tilde{0}_2\rangle_2 + e^{\frac{2\pi i}{3}}b|\tilde{1}_2\rangle_2, \\ |\tilde{\Psi}_3\rangle &\propto a|\tilde{0}_0\rangle_2 - b|\tilde{1}_0\rangle_2, \quad |\tilde{\Psi}_4\rangle \propto a|\tilde{0}_1\rangle_2 - e^{\frac{\pi i}{3}}b|\tilde{1}_1\rangle_2, \quad |\tilde{\Psi}_5\rangle \propto a|\tilde{0}_2\rangle_2 - e^{\frac{2\pi i}{3}}b|\tilde{1}_2\rangle_2. \end{aligned} \quad (\text{E5})$$

The final mixture for a logical qubit $|\bar{\Psi}\rangle = \frac{a|\bar{0}\rangle + b|\bar{1}\rangle}{\sqrt{1 + 2\text{Re}(a^*b\langle\bar{0}|\bar{1}\rangle)}}$ can thus be written in the form

$$\begin{aligned} \bar{\rho} = & p_0 \left[\frac{1 + 2\text{Re}(a^*b\langle\bar{0}_0|\bar{1}_0\rangle)}{1 + 2\text{Re}(a^*b\langle\bar{0}_0|\bar{1}_0\rangle)} \right] |\tilde{\Psi}_0\rangle\langle\tilde{\Psi}_0|, \\ & + p_1 \left[\frac{1 + 2\text{Re}(a^*be^{\frac{\pi i}{3}}\langle\bar{0}_1|\bar{1}_1\rangle)}{1 + 2\text{Re}(a^*b\langle\bar{0}_0|\bar{1}_0\rangle)} \right] |\tilde{\Psi}_1\rangle\langle\tilde{\Psi}_1|, \\ & + p_2 \left[\frac{1 + 2\text{Re}(a^*be^{\frac{2\pi i}{3}}\langle\bar{0}_2|\bar{1}_2\rangle)}{1 + 2\text{Re}(a^*b\langle\bar{0}_0|\bar{1}_0\rangle)} \right] |\tilde{\Psi}_2\rangle\langle\tilde{\Psi}_2|, \\ & + p_3 \left[\frac{1 - 2\text{Re}(a^*b\langle\bar{0}_0|\bar{1}_0\rangle)}{1 + 2\text{Re}(a^*b\langle\bar{0}_0|\bar{1}_0\rangle)} \right] |\tilde{\Psi}_3\rangle\langle\tilde{\Psi}_3|, \\ & + p_4 \left[\frac{1 - 2\text{Re}(a^*be^{\frac{\pi i}{3}}\langle\bar{0}_1|\bar{1}_1\rangle)}{1 + 2\text{Re}(a^*b\langle\bar{0}_0|\bar{1}_0\rangle)} \right] |\tilde{\Psi}_4\rangle\langle\tilde{\Psi}_4|, \\ & + p_5 \left[\frac{1 - 2\text{Re}(a^*be^{\frac{2\pi i}{3}}\langle\bar{0}_2|\bar{1}_2\rangle)}{1 + 2\text{Re}(a^*b\langle\bar{0}_0|\bar{1}_0\rangle)} \right] |\tilde{\Psi}_5\rangle\langle\tilde{\Psi}_5|, \quad (\text{E6}) \end{aligned}$$

where we also omitted the index indicating $L = 2$ at the state vectors. For this code, the code-word probabilities $p_i, i = 0, \dots, 5$, are given by

$$p_i = \frac{1}{\sqrt{N}} \sum_{m=0}^{\infty} \frac{[\alpha^2(1-\gamma)]^{6m+i}}{(6m+i)!}. \quad (\text{E7})$$

From the mixed final state in Eq. (E6), the nondeformation of the codewords becomes also manifest. Therefore, the KL conditions are approximately fulfilled. A recovery is therefore also approximately possible, provided the amplitudes are chosen large enough.

APPENDIX F: AMPLITUDE RESTORATION

One effect of the realistic photon-loss channel on the basic codewords is the damping of their amplitude. Consequently, the initial amplitude of the incoming logical state has to be restored.

The first step in our quantum-error correction process is a parity measurement that determines a certain error space. We have referred to this step as qubit recovery. For simplicity, the amplitude-damped codewords in the respective error space are denoted as $|\tilde{0}\rangle$ and $|\tilde{1}\rangle$ in the following. The goal of amplitude restoration, the second step of our QEC, is to turn back the damped amplitudes $\sqrt{\gamma}\alpha$ to the initial amplitude for every codeword, $|\tilde{0}\rangle \rightarrow |\bar{0}\rangle, |\tilde{1}\rangle \rightarrow |\bar{1}\rangle$. Later we will choose to map the qubit with restored amplitudes from the error space back into the code space (where this step is not a necessity, but helpful with respect to our one-way communication scheme).

Our strategy is to teleport the damped qubit into a space spanned by undamped codewords using an encoded, asymmetric Bell state with one half a damped qubit and the other half an undamped qubit [see Eq. (F10)]. In order to perform the Bell measurement onto a Bell basis expressed by nonorthogonal codewords, we propose to first apply a probabilistic ‘‘filter operation’’ and then do a standard Bell measurement. Let us now describe this filter [36]. Since the codewords are not orthogonal for finite α , they are not

perfectly distinguishable. However, they can be written in some orthonormal basis $\{|x\rangle, |y\rangle\}$ as

$$|\bar{0}\rangle = b_0|x\rangle + b_1|y\rangle, \quad |\bar{1}\rangle = e^{i\phi}(b_0|x\rangle - b_1|y\rangle), \quad (\text{F1})$$

where $b_0^2 + b_1^2 = 1$ and $b_0, b_1 \in \mathbb{R}$ with $b_0 > b_1$ without loss of generality. Furthermore, one has $\langle\bar{0}|\bar{1}\rangle = e^{i\phi}(2b_0^2 - 1)$, such that

$$b_0 = \sqrt{\frac{1 + e^{-i\phi}\langle\bar{0}|\bar{1}\rangle}{2}}, \quad b_1 = \sqrt{\frac{1 - e^{-i\phi}\langle\bar{0}|\bar{1}\rangle}{2}}. \quad (\text{F2})$$

Furthermore, we define the following operators:

$$A_s = \begin{pmatrix} \frac{b_1}{b_0} & 0 \\ 0 & 1 \end{pmatrix}, \quad A_f = \begin{pmatrix} \sqrt{1 - \left(\frac{b_1}{b_0}\right)^2} & 0 \\ 0 & 0 \end{pmatrix}. \quad (\text{F3})$$

As can easily be checked, one has $A_s^\dagger A_s + A_f^\dagger A_f = \mathbb{1}$ and we refer to the nonunitary operations expressed by A_s and A_f as a successful and a failed filter operation, respectively. A successful filter on the codewords leads to

$$A_s|\bar{0}\rangle = b_1(|x\rangle + |y\rangle), \quad (\text{F4})$$

$$A_s|\bar{1}\rangle = e^{i\phi}b_1(|x\rangle - |y\rangle);$$

i.e., it maps the nonorthogonal codewords onto orthogonal states. Because the codewords cannot be perfectly distinguished, this cannot be done deterministically. In fact, the success probability for the filter operation is

$$P_{\text{succ}} = \langle\bar{0}|A_s^\dagger A_s|\bar{0}\rangle = \langle\bar{1}|A_s^\dagger A_s|\bar{1}\rangle = 2 - 2b_0^2 = 1 - |\langle\bar{0}|\bar{1}\rangle|. \quad (\text{F5})$$

Before proceeding, we illustrate the idea using the $L = 0$ cat code, whose codewords are $|\bar{0}\rangle = |\alpha\rangle$ and $|\bar{1}\rangle = |-\alpha\rangle$ with real overlap $\langle\alpha|-\alpha\rangle = e^{-2\alpha^2}$. The corresponding orthogonal basis is the cat-state basis:

$$|x\rangle = \frac{1}{\sqrt{N_+}}(|\alpha\rangle + |-\alpha\rangle), \quad |y\rangle = \frac{1}{\sqrt{N_-}}(|\alpha\rangle - |-\alpha\rangle). \quad (\text{F6})$$

Since the overlap is real, we have $\phi = 0$ and find

$$b_0 = \sqrt{\frac{1 + \exp(-2\alpha^2)}{2}}, \quad b_1 = \sqrt{\frac{1 - \exp(-2\alpha^2)}{2}}. \quad (\text{F7})$$

The probability for successfully distinguishing $|\bar{0}\rangle$ and $|\bar{1}\rangle$ is therefore $P_{\text{succ}} = 1 - \exp(-2\alpha^2)$ (so-called unambiguous state discrimination).

For the teleportation-based amplitude restoration scheme, we need the Bell states in the (known) error space (note the normalization factor due to the nonorthogonality of the codewords):

$$\begin{aligned} |\tilde{\phi}_+\rangle &= \frac{1}{\sqrt{N_{\tilde{\phi}_+}}} \frac{|\tilde{0}\rangle|\tilde{0}\rangle + |\tilde{1}\rangle|\tilde{1}\rangle}{\sqrt{2}}, \\ |\tilde{\phi}_-\rangle &= \frac{1}{\sqrt{N_{\tilde{\phi}_-}}} \frac{|\tilde{0}\rangle|\tilde{0}\rangle - |\tilde{1}\rangle|\tilde{1}\rangle}{\sqrt{2}}, \\ |\tilde{\psi}_+\rangle &= \frac{1}{\sqrt{N_{\tilde{\psi}_+}}} \frac{|\tilde{0}\rangle|\tilde{1}\rangle + |\tilde{1}\rangle|\tilde{0}\rangle}{\sqrt{2}}, \\ |\tilde{\psi}_-\rangle &= \frac{1}{\sqrt{N_{\tilde{\psi}_-}}} \frac{|\tilde{0}\rangle|\tilde{1}\rangle - |\tilde{1}\rangle|\tilde{0}\rangle}{\sqrt{2}}. \quad (\text{F8}) \end{aligned}$$

For later use for the ‘‘Bennett decomposition’’ in the teleportation step, one rearranges the former equations into

$$\begin{aligned}
|\tilde{0}\rangle|\tilde{0}\rangle &= \frac{1}{\sqrt{2}}(\sqrt{N_{\tilde{\phi}_+}}|\tilde{\phi}_+\rangle + \sqrt{N_{\tilde{\phi}_-}}|\tilde{\phi}_-\rangle), \\
|\tilde{1}\rangle|\tilde{1}\rangle &= \frac{1}{\sqrt{2}}(\sqrt{N_{\tilde{\phi}_+}}|\tilde{\phi}_+\rangle - \sqrt{N_{\tilde{\phi}_-}}|\tilde{\phi}_-\rangle), \\
|\tilde{0}\rangle|\tilde{1}\rangle &= \frac{1}{\sqrt{2}}(\sqrt{N_{\tilde{\psi}_+}}|\tilde{\psi}_+\rangle + \sqrt{N_{\tilde{\psi}_-}}|\tilde{\psi}_-\rangle), \\
|\tilde{1}\rangle|\tilde{0}\rangle &= \frac{1}{\sqrt{2}}(\sqrt{N_{\tilde{\psi}_+}}|\tilde{\psi}_+\rangle - \sqrt{N_{\tilde{\psi}_-}}|\tilde{\psi}_-\rangle).
\end{aligned} \tag{F9}$$

The amplitude restoration works as follows. An encoded qubit is sent through the channel whose output is a mixed state. As pointed out in the main text, the first step in the error-correction procedure is the parity measurement which determines the corresponding error space; i.e., the input qubit of our amplitude restoration is of the form $|\omega\rangle = \frac{c_0|\tilde{0}\rangle + c_1|\tilde{1}\rangle}{\sqrt{N_\omega}}$ with unknown coefficients c_0 and c_1 . According to the result of the parity measurement, the following state must be generated:

$$|\hat{\phi}^+\rangle = \frac{1}{\sqrt{N_{\hat{\phi}^+}}} \frac{|\tilde{0}\rangle|\tilde{0}\rangle + |\tilde{1}\rangle|\tilde{1}\rangle}{\sqrt{2}}. \tag{F10}$$

In total, we then have

$$\begin{aligned}
|\omega\rangle \otimes |\hat{\phi}^+\rangle &= \frac{1}{\sqrt{N_\omega N_{\hat{\phi}^+}}} \frac{1}{\sqrt{2}} (c_0|\tilde{0}\rangle|\tilde{0}\rangle|\tilde{0}\rangle + c_0|\tilde{0}\rangle|\tilde{1}\rangle|\tilde{1}\rangle + c_1|\tilde{1}\rangle|\tilde{0}\rangle|\tilde{0}\rangle + c_1|\tilde{1}\rangle|\tilde{1}\rangle|\tilde{1}\rangle) \\
&= \frac{1}{\sqrt{N_\omega N_{\hat{\phi}^+}}} \frac{1}{2} [c_0\sqrt{N_{\tilde{\phi}_+}}|\tilde{\phi}_+\rangle|\tilde{0}\rangle + c_0\sqrt{N_{\tilde{\phi}_-}}|\tilde{\phi}_-\rangle|\tilde{0}\rangle + c_0\sqrt{N_{\tilde{\psi}_+}}|\tilde{\psi}_+\rangle|\tilde{1}\rangle + c_0\sqrt{N_{\tilde{\psi}_-}}|\tilde{\psi}_-\rangle|\tilde{1}\rangle \\
&\quad + c_1\sqrt{N_{\tilde{\psi}_+}}|\tilde{\psi}_+\rangle|\tilde{0}\rangle - c_1\sqrt{N_{\tilde{\psi}_-}}|\tilde{\psi}_-\rangle|\tilde{0}\rangle + c_1\sqrt{N_{\tilde{\phi}_+}}|\tilde{\phi}_+\rangle|\tilde{1}\rangle - c_1\sqrt{N_{\tilde{\phi}_-}}|\tilde{\phi}_-\rangle|\tilde{1}\rangle] \\
&= \frac{1}{\sqrt{N_\omega N_{\hat{\phi}^+}}} \frac{1}{2} [\sqrt{N_{\tilde{\phi}_+}}|\tilde{\phi}_+\rangle(c_0|\tilde{0}\rangle + c_1|\tilde{1}\rangle) + \sqrt{N_{\tilde{\phi}_-}}|\tilde{\phi}_-\rangle(c_0|\tilde{0}\rangle - c_1|\tilde{1}\rangle) \\
&\quad + \sqrt{N_{\tilde{\psi}_+}}|\tilde{\psi}_+\rangle(c_0|\tilde{1}\rangle + c_1|\tilde{0}\rangle) + \sqrt{N_{\tilde{\psi}_-}}|\tilde{\psi}_-\rangle(c_0|\tilde{1}\rangle - c_1|\tilde{0}\rangle)] \\
&= \frac{\sqrt{N_{\chi_1}}}{\sqrt{N_\omega N_{\hat{\phi}^+}}} \frac{1}{2} \sqrt{N_{\tilde{\phi}_+}}|\tilde{\phi}_+\rangle \left(\frac{c_0|\tilde{0}\rangle + c_1|\tilde{1}\rangle}{\sqrt{N_{\chi_1}}} \right) + \frac{\sqrt{N_{\chi_2}}}{\sqrt{N_\omega N_{\hat{\phi}^+}}} \frac{1}{2} \sqrt{N_{\tilde{\phi}_-}}|\tilde{\phi}_-\rangle \left(\frac{c_0|\tilde{0}\rangle - c_1|\tilde{1}\rangle}{\sqrt{N_{\chi_2}}} \right) \\
&\quad + \frac{\sqrt{N_{\chi_3}}}{\sqrt{N_\omega N_{\hat{\phi}^+}}} \frac{1}{2} \sqrt{N_{\tilde{\psi}_+}}|\tilde{\psi}_+\rangle \left(\frac{c_0|\tilde{1}\rangle + c_1|\tilde{0}\rangle}{\sqrt{N_{\chi_3}}} \right) + \frac{\sqrt{N_{\chi_4}}}{\sqrt{N_\omega N_{\hat{\phi}^+}}} \frac{1}{2} \sqrt{N_{\tilde{\psi}_-}}|\tilde{\psi}_-\rangle \left(\frac{c_0|\tilde{1}\rangle - c_1|\tilde{0}\rangle}{\sqrt{N_{\chi_4}}} \right) \\
&= \frac{\sqrt{N_{\chi_1}}}{\sqrt{N_\omega N_{\hat{\phi}^+}}} \frac{1}{2} \sqrt{N_{\tilde{\phi}_+}} \left(\frac{|\tilde{0}\rangle|\tilde{0}\rangle + |\tilde{1}\rangle|\tilde{1}\rangle}{\sqrt{2}} \right) \left(\frac{c_0|\tilde{0}\rangle + c_1|\tilde{1}\rangle}{\sqrt{N_{\chi_1}}} \right) \\
&\quad + \frac{\sqrt{N_{\chi_2}}}{\sqrt{N_\omega N_{\hat{\phi}^+}}} \frac{1}{2} \sqrt{N_{\tilde{\phi}_-}} \left(\frac{|\tilde{0}\rangle|\tilde{0}\rangle - |\tilde{1}\rangle|\tilde{1}\rangle}{\sqrt{2}} \right) \left(\frac{c_0|\tilde{0}\rangle - c_1|\tilde{1}\rangle}{\sqrt{N_{\chi_2}}} \right) \\
&\quad + \frac{\sqrt{N_{\chi_3}}}{\sqrt{N_\omega N_{\hat{\phi}^+}}} \frac{1}{2} \sqrt{N_{\tilde{\psi}_+}} \left(\frac{|\tilde{0}\rangle|\tilde{1}\rangle + |\tilde{1}\rangle|\tilde{0}\rangle}{\sqrt{2}} \right) \left(\frac{c_0|\tilde{1}\rangle + c_1|\tilde{0}\rangle}{\sqrt{N_{\chi_3}}} \right) \\
&\quad + \frac{\sqrt{N_{\chi_4}}}{\sqrt{N_\omega N_{\hat{\phi}^+}}} \frac{1}{2} \sqrt{N_{\tilde{\psi}_-}} \left(\frac{|\tilde{0}\rangle|\tilde{1}\rangle - |\tilde{1}\rangle|\tilde{0}\rangle}{\sqrt{2}} \right) \left(\frac{c_0|\tilde{1}\rangle - c_1|\tilde{0}\rangle}{\sqrt{N_{\chi_4}}} \right).
\end{aligned} \tag{F11}$$

Note that each of the four different output qubits requires a different normalization factor, which we denote as $N_{\chi_i}, i = 1, 2, 3, 4$. Like in a usual teleportation scheme, we have a superposition of tensor products of four Bell states and four different output qubits. Because the codewords $|\tilde{0}\rangle$ and $|\tilde{1}\rangle$ are not orthogonal, the Bell measurement in this basis cannot be performed deterministically. Therefore, we apply the filter operation on the first two modes individually which leads, after an additional Hadamard gate in

$\{|x\rangle, |y\rangle\}$, to

$$\begin{aligned}
 |\omega\rangle \otimes |\hat{\phi}^+\rangle &\rightarrow \frac{b_1^2 \sqrt{N_{\chi_1}} \sqrt{N_{\hat{\phi}^+}}}{\sqrt{N_{\omega} N_{\hat{\phi}^+}}} \left(\frac{|x\rangle|x\rangle + e^{2i\phi}|y\rangle|y\rangle}{\sqrt{2}} \right) \left(\frac{c_0|\tilde{0}\rangle + c_1|\tilde{1}\rangle}{\sqrt{N_{\chi_1}}} \right) + \frac{b_1^2 \sqrt{N_{\chi_2}} \sqrt{N_{\hat{\phi}^-}}}{\sqrt{N_{\omega} N_{\hat{\phi}^+}}} \left(\frac{|x\rangle|x\rangle - e^{2i\phi}|y\rangle|y\rangle}{\sqrt{2}} \right) \left(\frac{c_0|\tilde{0}\rangle - c_1|\tilde{1}\rangle}{\sqrt{N_{\chi_2}}} \right) \\
 &+ e^{i\phi} \frac{b_1^2 \sqrt{N_{\chi_3}} \sqrt{N_{\hat{\psi}^+}}}{\sqrt{N_{\omega} N_{\hat{\phi}^+}}} \left(\frac{|x\rangle|y\rangle + |y\rangle|x\rangle}{\sqrt{2}} \right) \left(\frac{c_0|\tilde{1}\rangle + c_1|\tilde{0}\rangle}{\sqrt{N_{\chi_3}}} \right) + e^{i\phi} \frac{b_1^2 \sqrt{N_{\chi_4}} \sqrt{N_{\hat{\psi}^-}}}{\sqrt{N_{\omega} N_{\hat{\phi}^+}}} \left(\frac{|x\rangle|y\rangle - |y\rangle|x\rangle}{\sqrt{2}} \right) \left(\frac{c_0|\tilde{1}\rangle - c_1|\tilde{0}\rangle}{\sqrt{N_{\chi_4}}} \right) \\
 &=: |\nu\rangle.
 \end{aligned} \tag{F12}$$

Note that compared to Eq. (F1) the $\{|x\rangle, |y\rangle\}$ basis is now that which expresses the damped states $|\tilde{0}\rangle$ and $|\tilde{1}\rangle$.

Since $|x\rangle$ and $|y\rangle$ are orthogonal, the Bell measurement can be performed. Because the filter operation is nondeterministic, the whole teleportation scheme has a nonunit success probability which corresponds to the norm of the state in Eq. (F12),

$$\begin{aligned}
 P_{\text{succ}} = \langle \nu | \nu \rangle &= \frac{b_1^4}{N_{\omega} N_{\hat{\phi}^+}} (N_{\chi_1} N_{\hat{\phi}^+} + N_{\chi_2} N_{\hat{\phi}^-} + N_{\chi_3} N_{\hat{\psi}^+} + N_{\chi_4} N_{\hat{\psi}^-}) \\
 &= \frac{(1 - b_0^2)^2}{N_{\omega} N_{\hat{\phi}^+}} (N_{\chi_1} N_{\hat{\phi}^+} + N_{\chi_2} N_{\hat{\phi}^-} + N_{\chi_3} N_{\hat{\psi}^+} + N_{\chi_4} N_{\hat{\psi}^-}) \\
 &= \frac{(1 - e^{-i\phi} \langle \tilde{0} | \tilde{1} \rangle)^2}{4N_{\omega} N_{\hat{\phi}^+}} (N_{\chi_1} N_{\hat{\phi}^+} + N_{\chi_2} N_{\hat{\phi}^-} + N_{\chi_3} N_{\hat{\psi}^+} + N_{\chi_4} N_{\hat{\psi}^-}) \\
 &= \frac{(1 - e^{-i\phi} \langle \tilde{0} | \tilde{1} \rangle)^2}{4[1 + 2 \text{Re}(c_0^* c_1 \langle \tilde{0} | \tilde{1} \rangle)] [1 + \text{Re}(\langle \tilde{0} | \tilde{1} \rangle \langle \tilde{0} | \tilde{1} \rangle)]} (N_{\chi_1} N_{\hat{\phi}^+} + N_{\chi_2} N_{\hat{\phi}^-} + N_{\chi_3} N_{\hat{\psi}^+} + N_{\chi_4} N_{\hat{\psi}^-}).
 \end{aligned} \tag{F13}$$

For an L -encoded qubit with coefficients a and b (i.e., now we replace $c_0 \rightarrow a$, $c_1 \rightarrow b$), the total success probability for the one-way scheme is (see Sec. V)

$$P_{ow} = \left\{ \sum_{k=0}^{2L+1} \tilde{p}_k(a, b) P_{\text{succ}} \left[a |\tilde{0}_k\rangle_L + \exp\left(\frac{k\pi i}{L+1}\right) b |\tilde{1}_k\rangle_L \right] \right\}^{\mathcal{L}/d_0}, \tag{F14}$$

where \mathcal{L} is the total distance, d_0 is the regular interval at which AR is performed, and the index “ k ” in the codewords is to be understood as modulo $L + 1$ to obtain the corresponding error space codewords (recall $q = 0, \dots, L$). Furthermore, $P_{\text{succ}}[\circ]$ is to be understood as P_{succ} from Eq. (F13) with the respective incoming qubit state \circ . Note that the sum goes over all components in the incoming mixed state because this probability does not correspond to the success probability of qubit QEC (as our QR is deterministic and imperfect, as expressed by the nonunit fidelity of the scheme) but to the probability for the filters (and hence each AR) to succeed.

Note that at every AR step, we may obtain one of four possible qubit states, as expressed by Eq. (F12). From the Bell measurement result it is known which one of the four. This “Pauli frame” can be recorded, however, without any additional operations, we may have an input qubit at the next station that differs from the original qubit at the sending station. For large α , this will not matter much in Eq. (F14) [see, e.g., $\tilde{p}_k(a, b)$ in Eq. (14)].

-
- [1] I. L. Chuang, D. W. Leung, and Y. Yamamoto, *Phys. Rev. A* **56**, 1114 (1997).
 [2] W. Wasilewski and K. Banaszek, *Phys. Rev. A* **75**, 042316 (2007).
 [3] S. Glancy, H. M. Vasconcelos, and T. C. Ralph, *Phys. Rev. A* **70**, 022317 (2004).
 [4] D. W. Leung, M. A. Nielsen, I. L. Chuang, and Y. Yamamoto, *Phys. Rev. A* **56**, 2567 (1997).
 [5] A. S. Fletcher, P. W. Shor, and M. Z. Win, [arXiv:0710.1052](https://arxiv.org/abs/0710.1052)
 [6] S. Muralidharan, J. Kim, N. Lütkenhaus, M. D. Lukin, and L. Jiang, *Phys. Rev. Lett.* **112**, 250501 (2014).
 [7] M. Bergmann and P. van Loock, *Phys. Rev. A* **94**, 012311 (2016).
 [8] D. Gottesman, A. Kitaev, and J. Preskill, *Phys. Rev. A* **64**, 012310 (2001).
 [9] M. Mirrahimi, Z. Leghtas, V. V. Albert, S. Touzard, R. J. Schoelkopf, L. Jiang, and M. H. Devoret, *New J. Phys.* **16**, 045014 (2014).
 [10] Z. Leghtas, G. Kirchmair, B. Vlastakis, R. J. Schoelkopf, M. H. Devoret, and M. Mirrahimi, *Phys. Rev. Lett.* **111**, 120501 (2013).
 [11] S. L. Braunstein, *Phys. Rev. Lett.* **80**, 4084 (1998).
 [12] S. Lloyd and Jean-Jacques E. Slotine, *Phys. Rev. Lett.* **80**, 4088 (1998).
 [13] S. L. Braunstein, *Nature (London)* **394**, 47 (1998).
 [14] P. van Loock, *J. Mod. Opt.* **57**, 1965 (2010).
 [15] T. Aoki, G. Takahashi, T. Kajiya, J.-i. Yoshikawa, S. L. Braunstein, P. van Loock, and A. Furusawa, *Nat. Phys.* **5**, 541 (2009).

- [16] J. Niset, J. Fiurášek, and N. J. Cerf, *Phys. Rev. Lett.* **102**, 120501 (2009).
- [17] More precisely, non-Gaussian logical states alone, such as logical qubits, are actually not enough to circumvent those no-go results when both error and recovery channels are of Gaussian nature [18]. Note that the amplitude-damping (photon-loss) channel is indeed a Gaussian channel. Nonetheless, non-Gaussian logical states subject to Gaussian error channels together with non-Gaussian ancilla states [8,19] or with non-Gaussian operations [9,10] for the recoveries do the trick. Similarly, Gaussian logical states subject to non-Gaussian error channels with only Gaussian recovery operations suffice to circumvent the no-go theorem [14,15].
- [18] R. Namiki, O. Gittsovich, S. Guha, and N. Lütkenhaus, *Phys. Rev. A* **90**, 062316 (2014).
- [19] S. Glancy and E. Knill, *Phys. Rev. A* **73**, 012325 (2006).
- [20] M. H. Michael, M. Silveri, R. T. Brierley, V. V. Albert, J. Salmilehto, L. Jiang, and S. M. Girvin, *Phys. Rev. X* **6**, 031006 (2016).
- [21] N. Ofek, A. Petrenko, R. Heeres, P. Reinhold, Z. Leghtas, B. Vlastakis, Y. Liu, L. Frunzio, S. M. Girvin, L. Jiang, M. Mirrahimi, M. H. Devoret, and R. J. Schoelkopf, *Nature* **536**, 441 (2016).
- [22] V. V. Albert, C. Shu, S. Krastanov, C. Shen, R.-B. Liu, Z.-B. Yang, R. J. Schoelkopf, M. Mirrahimi, M. H. Devoret, and L. Jiang, *Phys. Rev. Lett.* **116**, 140502 (2016).
- [23] T. C. Ralph, A. Gilchrist, G. J. Milburn, W. J. Munro, and S. Glancy, *Phys. Rev. A* **68**, 042319 (2003).
- [24] A. P. Lund, T. C. Ralph, and H. L. Haselgrove, *Phys. Rev. Lett.* **100**, 030503 (2008).
- [25] R. Wickert and P. van Loock, *Phys. Rev. A* **89**, 052309 (2014).
- [26] R. Wickert, N. K. Bernardes, and P. van Loock, *Phys. Rev. A* **81**, 062344 (2010).
- [27] M. A. Nielsen and I. L. Chuang, *Quantum Computation and Quantum Information: 10th Anniversary Edition*, 10th ed. (Cambridge University Press, New York, 2011).
- [28] In an optical fiber, one has $\gamma = \exp(-\frac{l}{L_{\text{att}}})$, where l is the propagation distance of the photon in the optical fiber and, typically, $L_{\text{att}} = 22$ km is the attenuation length.
- [29] Note that even for $L = 0$, i.e., when we consider the simple coherent state encoding $|\pm\alpha\rangle$ (see the notation for generalized cat codes in Sec. III), the resulting density matrix $\bar{\rho}$ intrinsically contains such a cyclic behavior [see Eq. (D17) for $L = 0$]. In this well-known case [3], the resulting mixture has only two terms, of which one corresponds to all even losses containing the initial (damped) qubit and the other one corresponds to all odd losses containing a phase-flipped version of the initial (damped) qubit. Since in either case, even or odd losses, the qubit lives in the same space spanned by the damped versions of $|\pm\alpha\rangle$, already a one-photon-loss error cannot be distinguished from zero loss and thus the qubit phase flip must be regarded as random.
- [30] Of course, we may also rewrite a logical (unnormalized) qubit initially expressed in the \bar{Z} basis, $|\bar{\Psi}\rangle = a|\bar{0}_+\rangle + b|\bar{1}_+\rangle$, as the same qubit expressed in the \bar{X} basis, $|\bar{\Psi}\rangle = \frac{a}{2}[(|\bar{0}_+\rangle + |\bar{1}_+\rangle) + (|\bar{0}_+\rangle - |\bar{1}_+\rangle)] + \frac{b}{2}[(|\bar{0}_+\rangle + |\bar{1}_+\rangle) - (|\bar{0}_+\rangle - |\bar{1}_+\rangle)] = \frac{a+b}{2}\sqrt{N_+}|\bar{0}_+ + \bar{1}_+\rangle + \frac{a-b}{2}\sqrt{N_-}|\bar{0}_+ - \bar{1}_+\rangle$. As said, this choice of basis leads to a deformation of the qubit for finite α (while the codewords are exactly orthogonal). Calculating the worst-case fidelity in this case is rather complicated, because every loss event leads to a differently deformed qubit in the resulting output density matrix.
- [31] D. Gottesman, [arXiv:quant-ph/9705052](https://arxiv.org/abs/quant-ph/9705052).
- [32] H.-J. Briegel, W. Dür, J. I. Cirac, and P. Zoller, *Phys. Rev. Lett.* **81**, 5932 (1998).
- [33] W. Dür, H.-J. Briegel, J. I. Cirac, and P. Zoller, *Phys. Rev. A* **59**, 169 (1999).
- [34] L. Jiang, J. M. Taylor, K. Nemoto, W. J. Munro, R. Van Meter, and M. D. Lukin, *Phys. Rev. A* **79**, 032325 (2009).
- [35] F. Ewert, M. Bergmann, and P. van Loock, [arXiv:1503.06777](https://arxiv.org/abs/1503.06777).
- [36] M. Dušek, M. Jahma, and N. Lütkenhaus, *Phys. Rev. A* **62**, 022306 (2000).